Radiative recombination from dark excitons in nanocrystals: Activation mechanisms and polarization properties

Anna V. Rodina and Alexander L. Efros

Phys. Rev. B **93**, 155427 — Published 22 April 2016

DOI: 10.1103/PhysRevB.93.155427

Radiative recombination from dark excitons: Activation mechanisms and polarization properties

Anna V. Rodina [1] and Alexander L. Efros [2]
[1] *Ioffe Institute, Russian Academy of Sciences, 194021 St. Petersburg, Russia and*
[2] *Naval Research Laboratory, Washington, DC 20375, USA*
(Dated: April 6, 2016)

We analyze theoretically physical mechanisms responsible for radiative recombination of the ground optically passive ("dark") exciton (DE), which dominates in photoluminescence (PL) of colloidal nanocrystals (NCs) at low temperatures. The DE becomes optically active due to its mixing with the bright excitons caused by an external magnetic field, dangling bond spins or by acoustic and optical phonons. These activation mechanisms mix the DE with different bright excitons and, consequently, lead to different PL polarization properties, because they are determined by dipole orientations of the bright excitons, which the DE is coupled with. We show that the PL polarization properties of prolate and oblate shape NCs are different due to different activation mechanisms responsible for the DE recombination.

PACS numbers: 78.67.-n, 78.67.Bf, 73.21.La, 78.55.Et

I. INTRODUCTION

In all bulk semiconductors and all existing semiconductor hetero-structures a ground exciton state is without known exception an optically passive "dark" exciton (DE). The direct optical excitation of this state by a single photon or its direct photon emission is forbidden due to the parallel alignment of the electron and hole spins caused by ferromagnetic character of the electron-hole exchange interaction. Interaction with light affects only the orbital degrees of freedom of valence and conduction band electrons, and does not change the electron spin projection. As a result of this, only exciton states with anti-parallel alignment of the electron and hole spins ("bright" exciton states) could be excited directly by a photon and directly emit a photon.

The DE recombination does not significantly affect photoluminescence (PL) in commonly used bulk semiconductors or epitaxial quantum dots and quantum wires, due to small energy splitting between bright and dark excitons. This splitting in bulk semiconductors, where it is called singled-triplet splitting,[1] epitaxial quantum wells,[2,3] and quantum dots,[4–6] is usually (with several rare exceptions[7–9]) smaller than the helium temperatures and inhomogeneous exciton line-width. This is not a case however for small colloidal nanocrystals (NCs), nanorods and nanoplatelets, where the strong spatial confinement leads to the dark-bright exciton splitting on the order dozens meVs.[10–18] In such nano-structures the radiative recombinations of the DE dominates PL at low temperatures.

The DE can recombine radiative via some assisting processes, which mix the DE to some optically active bright exciton state. The activation processes mix up or flip different electron or hole spin projections causing a virtual transition of the DE to the bright exciton state, which subsequently decays radiatively. These processes are much slower than direct optical recombination of bright excitons and are accurately described by second order perturbation theory.[11,13] In colloidal NCs, the radiative recombination of DEs at low temperatures was observed directly in fluorescence line narrowing (FLN) experiments[12,19–25] and in single dot (SD) experiments.[26–31] Optical transitions assisted by optical and acoustic phonons as well as the zero phonon line (ZPL) were identified in low temperature PL. Evidence for DE radiative recombination was also observed by time–resolved PL measurements due to the presence of the slow decaying component at cryogenic temperatures.[18,27,28,32–41]

The magnetic field activation of the ZPL intensity and shortening of its life time is observed in all kinds of FLN, SD and time–resolved experiments and well explained theoretically.[11,13] However, the mechanism of the ZPL activation in zero magnetic field remains the subject of discussions. The finite radiative life time of the lowest dark exciton states was obtained, for example, by the atomistic pseudopotential[14,42] and tight–bidning[43] calculations. It was suggested[44] that a decrease of the geometrical symmetry of colloidal NCs below C_{6v} , at which they have ellipsoidal shape with rotation axis directed along the hexagonal c-axis of wurtzite semiconductor, also results in DE activation. The strong asymmetry of the NC shape, however, is required because only very untypical faceting of the cubic or wutzite NC reduces the NC symmetry below C_{6v} . Recently,[45] the activation of the DE by the interaction with free spins of the dangling bonds at the NC surface was considered theoretically. Existence of the dangling bond spins at the NC surfaces and their magnetization by an external magnetic field was demonstrated by SQUID measurements.[46,47] The dangling bond spin–flip assisted recombination was shown to be suppressed by the formation of the magnetic polaron state with decreasing temperature explaining the temperature dependence of the ZPL position and intensity observed experimentally.[20]

It is important to note, that the polarization properties of the DE PL are controlled by the polarization of

the bright exciton which contributes to the DE recombination via some assisting process.[45,48] That is why a study of the DE PL polarization could be a powerful tool for revealing the physical mechanisms responsible for the DE radiative recombination and the fine structure of the band edge exciton.[48,49]

In this article we consider and compare theoretically four mechanisms of activation of the DE in ellipsoidal shape NCs made from semiconductors which have cubic or wurzite lattice structures. These mechanisms include the interactions with dangling-bond spins at the NC surface, acoustic and optical phonon assisted recombination, as well as external magnetic field induced recombination of the DE. We show that dangling-bond spin and phonon assisted mechanisms lead to different polarizations of the DE PL and thus might be identified experimentally. For example, in CdSe NCs with the ± 2 ground DE the dangling bond spin assisted recombination results in PL which is circularly polarized around the NC c-axis, while in the case of phonon assisted recombination the PL is mostly linearly polarized along the NC c-axis. These results suggest that dangling bonds are responsible for the DE recombination in CdSe NCs where SD experiments demonstrated that DEs have properties of the degenerate 2D dipole oriented isotropically in two dimensions perpendicular to the NC hexagonal axis at low[50] as well as at room[51,52] temperatures. On the other hand, at very low temperatures when the dangling bond assisted recombination is suppressed in small size NCs by the formation of the polaron state,[45] the DE decays via acoustic or optical phonons and the PL should be strongly polarized linearly along c-axis. This explains[48] the negative polarization memory effect measured in CdSe NC ensembles after resonant excitation of the lowest bright exciton state.[12,21] Calculations also show that in contrast to the ± 2 DE, the $0^{\rm L}$ DE can be activated by an external magnetic field parallel to the c-axis of CdSe NCs and that an external magnetic field activates the DE in even spherical or "quasi-spherical" NCs.

This paper is organized as follows: in Sec. II we introduce the Hamiltonian that describes the exciton fine structure, describe the most general form of perturbations that could activates the DE, and discuss the interaction of excitons with light in the dipole approximation. In Sec. III we consider four activation mechanisms of the ± 2 ground DE. In section IV we discuss the magnetic field induced activation of the degenerate $\mathcal{F}=2$ ground DE in spherical or "quasi-spherical" NCs. Sec. V summarizes the results for the four activation mechanisms of the $0^{\rm L}$ ground DE. The main theoretical conclusions and comparison with available experimental data are presented in Sec. VI. Supporting details for calculations are given in Appendix.

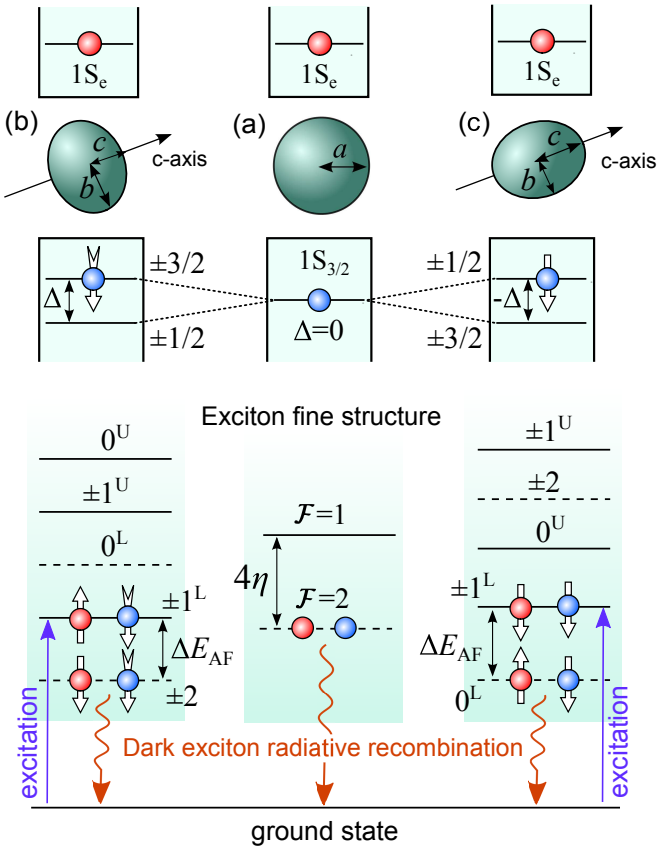

FIG. 1: Schematic image of the holes energy spectrum and the fine structure of the band edge excitons. Panel (a) describes spherical NCs with cubic lattice structure and radius a and "quasi-spherical" wurtzite CdSe NCs, panel (b) describes oblate ellipsoidal shape CdSe NCs with short semi axis $c < b$, and panel (c) describes prolate CdSe NCs with long semi axis $c > b$. The total energy splitting Δ is caused by the wurtzite crystal field and NC shape anisotropy and is zero in (a), positive in (b) and negative in (c). As a result, dark ± 2 exciton states are formed with heavy holes $\pm 3/2$ (b), while the $0^{\rm L}$ DE state is formed with light holes $\pm 1/2$ (c). The states with total momentum $\mathcal{F}=2$ and $\mathcal{F}=1$ in spherical or "quasi-spherical" NCs are separated by the electron–hole exchange interaction $4\eta \propto 1/a^3$. Bright and dark exciton levels are shown in (a), (b) and (c) by solid and dashed lines, respectively.

II. EXCITON FINE STRUCTURE AND DARK EXCITON ACTIVATION MECHANISMS

Let us discuss briefly the fine structure of the band-edge exciton in NCs made of direct-gap semiconductors with band edges in Γ points of Brillouin zone. In spherically symmetric NCs made of direct gap $\rm A_{II}B_{VI}$ and $\rm A_{III}B_{V}$ semiconductors with cubic lattice structure, the electron ground $1S_{\rm e}$ level is doubly degenerate with respect to its spin projection, $s_z = \pm 1/2$ and the hole ground $1S_{3/2}$ level is 4-fold degenerate with respect to projections $M = 3/2$, $1/2$, $-1/2$, and $-3/2$ of its total angular momentum, $J = 3/2$.[53,54] As a result the

absorption band edge and the PL of these NCs are determined by the 8=4x2 optical exciton transitions between these lowest electron and hole levels. The electron-hole exchange interaction splits the 8-fold degenerate exciton state in spherical NCs into the ground optically passive (dark) 5–fold degenerate state with total momentum $\mathcal{F} = 2$ and the upper optically active 3–fold degenerate state with $\mathcal{F} = 1$ by the energy 4η, where the exchange constant $\eta \propto 1/a^3$ and a is the NC radius. For the short–range exchange interaction the exchange constant is defined in Refs.[11,55] (see also Appendix A). The two-level exciton structure of spherical cubic NCs is shown schematically in Fig. 1(a).

The spherical symmetry can be broken by the internal hexagonal crystal field in semiconductors with wurtzite structures (such as CdSe) and the non-spherical, ellipsoidal shape of NCs. These two effects split $M = \pm 3/2$ and $M = \pm 1/2$, so called "heavy" and "light" hole sublevels, by[11] $\Delta = \Delta_{\rm int} + \Delta_{\rm sh}$ and finally results in the five band edge exciton states, $F = \pm 2, \pm 1^{L,U}, 0^{L,U}$ with different projections, $F = M + s_z$, on the hexagonal c-axis of the NC. The resulting fine structure of the exciton levels is described by the following Hamiltonian:[11]

$$\hat{H}_{\rm fine} = -\eta(\boldsymbol{\sigma}^{\rm e}\boldsymbol{J}) + \frac{\Delta}{2}\left[5/4 - M^2\right] , \qquad (1)$$

where $\boldsymbol{\sigma}^{\rm e}$ is the electron spin Pauli matrix. The energies and wave functions of the above mentioned dark and bright band edge excitons were derived in Ref. [11] and for convenience we show them again in the Appendix A. The calculations show that the exciton fine structure depends strongly on the size and shape of the NC as shown schematically in Fig. 1. The levels are labeled by the projection of the exciton total angular momentum F: one level with $F = \pm 2$, two with $F = \pm 1$, and two with $F = 0$. In the case when $\Delta \neq 0$, both of the ± 1 states (lower $1^{\rm L}$ and upper $1^{\rm U}$) are optically active bright excitons. For the states with $F = 0$ only the upper one, $0^{\rm U}$, is optically active, while the lower one, $0^{\rm L}$, is the optically passive DE. In oblate and spherical wurtzite CdSe NCs $\Delta > 0$ and the ground dark exciton is the state with $F = \pm 2$ (see Fig. 1(b)). In prolate CdSe NCs where $\Delta < 0$ the ground DE has $F = 0$ (see Fig. 1(c)). The two level structure of spherical NCs (see Fig. 1(a)) could be also realized in prolate wurtzite CdSe NCs. The negative value of $\Delta_{\rm sh}$ could result in $\Delta = 0$ in prolate CdSe NCs of a certain size, which will be called later "quasi-spherical".[11]

Thus the ground exciton state is always optically passive DE in all three cases shown in Fig. 1. Calculations show that in small CdSe NCs a typical energy splitting between the ground dark exciton and the lowest optically active (bright) exciton state, which are denoted in Fig. 1 as $\Delta E_{\rm AF}$, is on the order 10–20 meV.[11] As a result only the DE contributes to the NC photoluminescence (PL) at low temperatures.

Let us consider activation mechanisms of the ground DEs for all possible level structures shown schematically in Fig. 1. These mechanisms should provide the mixing of the bright exciton states into a DE state via either the flip the electron spin caused by some perturbation $\hat{V}_{\rm e}$ or the mixing of the hole states caused by some perturbation $\hat{V}_{\rm h}$. We consider the total spin Hamiltonian describing the band edge excitons in NCs with direct account of the electron-hole exchange interaction, hexagonal anisotropic field and additional mixing perturbations as

$$\hat{H}_{\rm spin} = \hat{H}_{\rm fine} + \hat{V}_{\rm e} + \hat{V}_{\rm h} . \qquad (2)$$

It can be written explicitly in the form of the 8x8 matrix in the bases of the two $\uparrow \equiv 1/2$ and $\downarrow \equiv -1/2$ electron states and the four $M = \pm 1/2, \pm 3/2$ hole states (the electron, $\Psi^{\rm e}_{\pm 1/2}$, and hole, $\Psi^{\rm h}_{M}$, wave functions for these states are given in Appendix A):

$$
\begin{array}{c}
 \\
\uparrow,3/2 \\
\uparrow,1/2 \\
\uparrow,-1/2 \\
\uparrow,-3/2 \\
\downarrow,3/2 \\
\downarrow,1/2 \\
\downarrow,-1/2 \\
\downarrow,-3/2
\end{array}
\begin{array}{c}
\begin{array}{cccccccc}
\uparrow,3/2 & \uparrow,1/2 & \uparrow,-1/2 & \uparrow,-3/2 & \downarrow,3/2 & \downarrow,1/2 & \downarrow,-1/2 & \downarrow,-3/2
\end{array} \\
\left(\begin{array}{cccccccc}
-\frac{3\eta}{2}-\frac{\Delta}{2} & V_{\rm h,1} & V_{\rm h,2} & 0 & V_{\rm e} & 0 & 0 & 0 \\
+V_{\uparrow,3/2} & & & & & & & \\
V_{\rm h,1}^* & -\frac{\eta}{2}+\frac{\Delta}{2} & V_{\rm lh} & 0 & \sqrt{3}\eta & V_{\rm e} & 0 & 0 \\
 & +V_{\uparrow,1/2} & & & & & & \\
V_{\rm h,2}^* & V_{\rm lh}^* & \frac{\eta}{2}+\frac{\Delta}{2} & 0 & 0 & 2\eta & V_{\rm e} & 0 \\
 & & +V_{\uparrow,-1/2} & & & & & \\
0 & 0 & 0 & \frac{3\eta}{2}-\frac{\Delta}{2} & 0 & 0 & \sqrt{3}\eta & V_{\rm e} \\
 & & & +V_{\uparrow,-3/2} & & & & \\
V_{\rm e}^* & \sqrt{3}\eta & 0 & 0 & \frac{3\eta}{2}-\frac{\Delta}{2} & V_{\rm h,1} & V_{\rm h,2} & 0 \\
 & & & & +V_{\downarrow,3/2} & & & \\
0 & V_{\rm e}^* & 2\eta & 0 & V_{\rm h,1}^* & \frac{\eta}{2}+\frac{\Delta}{2} & V_{\rm lh} & 0 \\
 & & & & & +V_{\downarrow,1/2} & & \\
0 & 0 & V_{\rm e}^* & \sqrt{3}\eta & V_{\rm h,2}^* & V_{\rm lh}^* & -\frac{\eta}{2}+\frac{\Delta}{2} & 0 \\
 & & & & & & +V_{\downarrow,-1/2} & \\
0 & 0 & 0 & V_{\rm e}^* & 0 & 0 & 0 & -\frac{3\eta}{2}-\frac{\Delta}{2} \\
 & & & & & & & +V_{\downarrow,-3/2}
\end{array}\right)
\end{array}
\tag{3}
$$

The admixture of the bright exciton states $\pm 1^{\rm L,U}, 0^{\rm U}$ into the DE $\pm 2, 0^{\rm L}$ states is mediated by at least one of four matrix elements: $V_{\rm e} = \langle 1/2|\hat{V}_{\rm e}|-1/2\rangle$ for the flip of the electron spin and $V_{\rm lh} = \langle \Psi_{+1/2}|\hat{V}_{\rm h}|\Psi_{-1/2}\rangle$, $V_{\rm h,1} = \langle \Psi_{+3/2}|\hat{V}_{\rm h}|\Psi_{+1/2}\rangle$ and $V_{\rm h,2} = \langle \Psi_{+3/2}|\hat{V}_{\rm h}|\Psi_{-1/2}\rangle$ for the mixing wave functions of the hole ground state, Ψ_M, with initial and final hole momentum projections, M, differing by ± 1 or ± 2. The matrix elements $V_{\rm e}$, $V_{\rm lh}$ and $V_{\rm h,1}$ can be provided by the external magnetic field perpendicular to the c-axis[11,13] or by the exchange interaction with the spin of dangling bonds at the NC surface.[45] The interactions with optical or acoustic phonons with angular momentum 2 provide the hole state mixing described by $V_{\rm h,1}$ and $V_{\rm h,2}$.[56–58] In addition, the diagonal matrix elements $V_{\uparrow(\downarrow),M} = \langle \Psi_{\uparrow(\downarrow),M}|\hat{V}_{\rm e} + \hat{V}_{\rm h}|\Psi_{\uparrow(\downarrow),M}\rangle$ of the $\hat{V}_{\rm e}$ or $\hat{V}_{\rm h}$ perturbations, e.g. external magnetic field or crystal field or stress along the c-axis, may result in activation of $\pm 1^{\rm L}$ and $0^{\rm L}$ excitons by their admixture to the $\pm 1^{\rm U}$ and $0^{\rm U}$ excitons without a flip of either hole or electron spins. The mixing of the $\pm 1^{\rm L}$ DE to the $\pm 1^{\rm U}$ bright exciton by the crystal field is the well known example of such activation.

The resulting probability of the DE radiative recombination can be found in the framework of the second order perturbation theory,[11,13,45] which describes a virtual transition of the DE to the bright exciton states $\pm 1^{\rm L,U}, 0^{\rm U}$ and its consequential radiative decay. The polarization of the DE emission is defined by the polarization properties of the corresponding bright excitons. Therefore, we start with a review of previously discussed[11,13] probabilities of the bright excitons radiative emission and polarization of corresponding optical transitions.

In the dipole approximation, the exciton interaction with light is described by the perturbation $q/(m_0\omega)\boldsymbol{E}\hat{\boldsymbol{p}}$, where $\boldsymbol{E} = E[\exp(-i\omega t)\boldsymbol{e} + \exp(i\omega t)\boldsymbol{e}^*]$ is the electric field of the light, q and m_0 are the free electron charge and mass, respectively, ω is the light frequency, E is the amplitude of the electric field, $\boldsymbol{e}$ is the light polarization vector and $\hat{\boldsymbol{p}} = -i\hbar\nabla$ is the momentum operator acting only on the valence band and conduction band Bloch functions.[59,60] The momentum matrix elements $\boldsymbol{d} = \langle {\rm G}|\hat{\boldsymbol{p}}|{\rm X}\rangle$ between the unexcited ground state G of the NC and the band-edge exciton state X are related to the matrix elements $\boldsymbol{d} = \langle {\rm G}|q\hat{\boldsymbol{r}}|{\rm X}\rangle$ of the dipole operator $q\hat{\boldsymbol{r}}$ as[60] $\boldsymbol{d} = im_0(E_{\rm g}/q\hbar)\tilde{\boldsymbol{d}}$, where $E_{\rm g}$ is the gap energy of the bulk semiconductor. This connection allows us hereafter to call $\boldsymbol{d}$ the dipole transition matrix elements. They are not zero only for the bright exciton states, which are ${\rm X} = \pm 1^{\rm L,U}, 0^{\rm U}$. The bright exciton state $0^{\rm U}$ is polarized along the c-axis of the NC. For this state, the square of projections of corresponding dipole transition elements are $|d_\perp|^2 = |d_x|^2 = |d_y|^2 = 0$ and $|d_0|^2 \equiv |d_\parallel|^2 = |d_z|^2 = |\langle {\rm G}|\hat{p}_z|0^{\rm U}\rangle|^2 = 4P^2K/3$, where both the Kane matrix element of the band-to-band transitions in zinc blende or wurtzite semiconductors in the quasi–cubic approximation, P, and the electron–hole wave functions overlap integral squared, K, are defined in Appendix A. The linear polarized dipole is often referred to as the nondegenerate 1D dipole.[51]

The bright exciton states $\pm 1^{\rm U,L}$ are polarized perpendicular to the c-axis and are usually referred to as the degenerate 2D dipoles.[50–52] The square of projections of the dipole transition matrix elements are $|d_\parallel^{\pm 1}|^2 = 0$ and

$|d_{\perp}^{\mathrm{U,L}}|^2 = |d_{+1}^{\mathrm{U,L}}|^2 + |d_{-1}^{\mathrm{U,L}}|^2$, where

$$d_{\pm 1}^{\mathrm{U}} = \frac{1}{2}\langle G|\hat{p}_x \pm ip_y|\pm 1^{\mathrm{U}}\rangle = \mp\frac{d_0}{2\sqrt{2}}\left(C^{+} + \sqrt{3}C^{-}\right),$$
$$d_{\pm 1}^{\mathrm{L}} = \frac{1}{2}\langle G|\hat{p}_x \pm ip_y|\pm 1^{\mathrm{L}}\rangle = \frac{d_0}{2\sqrt{2}}\left(\sqrt{3}C^{+} - C^{-}\right). \quad (4)$$

and the constants $C^{\pm}$, introduced in Ref. 11, are defined in Appendix A. It is easy to show that in any NC the sum $|d_{\perp}|^2 = |d_{\perp}^{\mathrm{L}}|^2 + |d_{\perp}^{\mathrm{U}}|^2 = |d_0|^2 = |d_{\parallel}|^2$. In the spherical and "quasi-spherical" NCs with $\Delta = 0$ the coefficients $C^{+} = 1/2$ and $C^{-} = \sqrt{3}/2$, so that the $\pm 1^{\mathrm{L}}$ excitons become the DEs.

According to the Fermi's "golden rule", the probability of the spontaneous emission of the $\boldsymbol{e}$ -polarized photon is given by

$$\Gamma_{\boldsymbol{e}} = \frac{2\pi}{\hbar}\frac{e^2}{m_0^2\omega^2}|\boldsymbol{E}^{\mathrm{int}}\boldsymbol{d}|^2\rho(\omega)\,, \quad (5)$$

where $\rho(\omega)$ is the density of the photon states and $\boldsymbol{E}^{\mathrm{int}} = E^{\mathrm{int}}\boldsymbol{e}^{*}$ is the electric field of the photon inside the NC which is different from its electric field $\boldsymbol{E}^{\mathrm{out}}$ in the outside medium due to the local field effect.[48,61–65] The total radiative rate can be obtained after the averaging over all possible polarizations as

$$\frac{1}{\tau} = \int_0^{\pi}\Gamma_{\boldsymbol{e}}\sin\Theta_{\boldsymbol{e}}d\Theta_{\boldsymbol{e}} = \frac{4e^2\omega n}{3\hbar m_0^2c^3}\left(D_{\parallel}|d_{\parallel}|^2 + 2D_{\perp}|d_{\perp}|^2\right), \quad (6)$$

where $\Theta_{\boldsymbol{e}}$ is the angle between $\boldsymbol{e}$ and c -axis (chosen as the z direction), n is the refractive index of the medium outside the NC, and factors $D_{\perp} = |E_{x,y}^{\mathrm{in}}|^2/|E_{x,y}^{\mathrm{out}}|^2$ and $D_{\parallel} = |E_z^{\mathrm{in}}|^2/|E_z^{\mathrm{out}}|^2$ are the local field screening factors.

As a result the radiative rate of the 0^{U} bright exciton is[11,13,66]

$$\frac{1}{\tau_0} = \frac{4e^2\omega n}{3\hbar m_0^2c^3}D_{\parallel}|d_0|^2 = \frac{16e^2\omega n}{9\hbar m_0^2c^3}D_{\parallel}P^2K\,. \quad (7)$$

The relations of Eqs. (4) allow us to express the dipole transition matrix elements and radiative rates of all excitons hereafter via $|d_0|^2$ and $1/\tau_0$.

For the DE states $\mathrm{X} = \pm 2, 0^{\mathrm{L}}$, the dipole transitions matrix elements are zero in first order perturbations theory. However, the admixture of the bright $\pm 1^{\mathrm{U,L}}$ and 0^{U} excitons into the DE may result in nonzero $|d_{\perp}^{\mathrm{DE}}|^2$ and $|d_{\parallel}^{\mathrm{DE}}|^2$ in second order perturbations theory. The radiative emission rate of the DE is described then by Eq. (6) with $|d_{\perp}|^2 = |d_{\perp}^{\mathrm{DE}}|^2$ and $|d_{\parallel}|^2 = |d_{\parallel}^{\mathrm{DE}}|^2$ calculated for the DE and can be written in the following form

$$\Gamma_{\mathrm{DE}} = \frac{1}{\tau_0}\left(\frac{|d_{\parallel}^{\mathrm{DE}}|^2}{|d_0|^2} + 2\frac{D_{\perp}}{D_{\parallel}}\frac{|d_{\perp}^{\mathrm{DE}}|^2}{|d_0|^2}\right). \quad (8)$$

The polarization properties of the DE emission can be characterized by the anisotropy parameter[48,49] $r_{\mathrm{d}} = Rf_{\mathrm{d}}$, which is a product of a parameter $R = D_{\parallel}/D_{\perp}$ that describes the anisotropy of the local field effect, and the parameter $f_{\mathrm{d}} = |d_{\parallel}^{\mathrm{DE}}|^2/|d_{\perp}^{\mathrm{DE}}|^2$ that describes anisotropy of the dipole matrix elements. The last one depends on the physical mechanism responsible for the DE activation. Note, that in the spherical NCs, the local field effect becomes isotropic and $R = 1$.

In the following sections we calculate $|d_{\parallel}^{\mathrm{DE}}|^2$ and $|d_{\perp}^{\mathrm{DE}}|^2$ and find the rate of the DE radiative recombination and its anisotropy for several mechanisms of the DE activation. The total radiative recombination rate of the DE can be written as sum of their contributions:

$$\Gamma_{\mathrm{DE}} = \Gamma_{\mathrm{ph}} + \Gamma_{\mathrm{db}} + \Gamma_B\,, \quad (9)$$

where $\Gamma_{\mathrm{ph}} = \Gamma_{\mathrm{LO}} + \Gamma_{\mathrm{AC}}$ is the phonon assisted radiative decay rate due to the interaction with optical (Γ_{LO}) and/or acoustic (Γ_{AC}) phonons, the ZPL recombination rate Γ_{db} is associated with the dangling bond assisted radiative recombination and Γ_B is the magnetic field induced recombination rate. In this paper we consider all activation mechanisms as independent, neglecting, for example, such effect as the alignment of the dangling bond spins by an external magnetic field.

III. RADIATIVE RECOMBINATION OF THE ± 2 DARK EXCITON

Let us calculate the matrix elements that mix up bright excitons and the ± 2 DE and lead to its radiative decay. It is clear from Eq. (3) that perturbations V_{e} and $V_{\mathrm{h},1}$ couple the ± 2 dark exciton with the $\pm 1^{\mathrm{L,U}}$ bright exciton states resulting in $d_{\perp}^{\pm 2}$, while $V_{\mathrm{h},2}$ couples the ± 2 exciton only with the 0^{U} bright state resulting in $d_{\parallel}^{\pm 2}$. Using the exciton wave functions in Eq. (40) from Appendix A and Eq. (3) we find matrix elements that describe the couplings:

$$\begin{aligned}
\langle -1^{\mathrm{U,L}}|\hat{V}_{\mathrm{e}}|-2\rangle &= C^{\mp}V_{\mathrm{e}}\,,\\
\langle +1^{\mathrm{U,L}}|\hat{V}_{\mathrm{e}}|+2\rangle &= \mp C^{\mp}V_{\mathrm{e}}^{*}\,,\\
\langle -1^{\mathrm{U,L}}|\hat{V}_{\mathrm{h}}|-2\rangle &= \mp C^{\pm}V_{\mathrm{h},1}\,,\\
\langle +1^{\mathrm{U,L}}|\hat{V}_{\mathrm{h}}|+2\rangle &= C^{\pm}V_{\mathrm{h},1}^{*}\,,\\
\langle 0^{\mathrm{U}}|\hat{V}_{\mathrm{h}}|-2\rangle &= -\frac{V_{\mathrm{h},2}}{\sqrt{2}}\,,\\
\langle 0^{\mathrm{U}}|\hat{V}_{\mathrm{h}}|+2\rangle &= \frac{V_{\mathrm{h},2}}{\sqrt{2}}^{*}\,.
\end{aligned} \quad (10)$$

Equations (10) allow us to calculate the squares of the dipole transition matrix elements for the ± 2 DE in second order perturbation theory. Using the dipoles of the bright $\pm 1^{\mathrm{L,U}}, 0^{\mathrm{U}}$ excitons defined in Eq. (4) and matrix

Coupling to	$\pm1^{\rm L,U}$ states	Coupling to $0^{\rm U}$ state
Polarization	$\perp \boldsymbol{c}$-axis	$\parallel \boldsymbol{c}$-axis
Dipole element	$\lvert d_\perp^{\pm2}\rvert^2 = \lvert d_0\rvert^2 \cdot \chi_\alpha^{21}$	$\lvert d_\parallel^{\pm2}\rvert^2 = \lvert d_0\rvert^2 \cdot \chi_\alpha^{20}$
Radiative rate	$\Gamma_\alpha^{21} = \frac{2}{R}\frac{1}{\tau_0}\cdot\chi_\alpha^{21}$	$\Gamma_\alpha^{20} = \frac{1}{\tau_0}\cdot\chi_\alpha^{20}$
Mechanism (α)	χ_α^{21}	χ_α^{20}
Magnetic field (B)	$\frac{[g_{\rm e}\mu_{\rm B}B\sin\Theta]^2}{96\eta^2}$	
Dangling bonds (db)	$\frac{\alpha^2}{12\eta^2}N_{\rm db}\left[1-\rho_{\rm ex}\rho_{\rm db}\right]$	
Acoustical phonons (AC)		$\frac{V_{\rm AC}^2}{2(\Delta+4\eta)^2}\coth\frac{E_{\rm AC}}{2kT}$
Optical phonons (LO)	$\frac{V_{\rm LO}^2E_{\rm LO}^2}{8(3\Delta\eta+E_{\rm LO}(\Delta+4\eta)+E_{\rm LO}^2)^2}$	$\frac{V_{\rm LO}^2}{2(\Delta+4\eta+E_{\rm LO})^2}$

TABLE I: Radiative decay rates and polarization properties of the ±2 DE activated by various physical mechanisms. For activation caused by magnetic field (B), dangling bonds (db), acoustic (AC) and optical (LO) phonons, the squares of the dipole transition matrix elements, $|d_\perp^{\pm2}|^2 = |d_0|^2\chi_\alpha^{21}$ and $|d_\parallel^{\pm2}|^2 = |d_0|^2\chi_\alpha^{20}$, induced by the coupling of the ±2 DE with $\pm1^{\rm U}$ and $0^{\rm U}$ bright excitons, respectively, where $\alpha = B, {\rm db}, {\rm AC}$ and LO. The radiative recombination rates induced by these activation mechanisms can be written correspondingly $\Gamma_\alpha^{21} = 2\chi_\alpha^{21}/(R\tau_0)$ and $\Gamma_\alpha^{20} = \chi_\alpha^{20}/(\tau_0)$.

elements of Eqs. (10) we find the following expressions:

$$|d_\parallel^{\pm2}|^2 = \frac{|d_0|^2}{2}\frac{|V_{\rm h,2}|^2}{(\tilde\varepsilon_0^U-\tilde\varepsilon_{\pm2})^2}, \quad (11)$$

$$|d_\perp^{\pm2}|^2 = \frac{|d_0|^2}{8}\left|\frac{(C^-V_{\rm e}-C^+V_{\rm h,1})(C^++\sqrt{3}C^-)}{\tilde\varepsilon_{\pm1}^{\rm U}-\tilde\varepsilon_{\pm2}} + \frac{(C^+V_{\rm e}+C^-V_{\rm h,1})(\sqrt{3}C^+-C^-)}{\tilde\varepsilon_{\pm1}^{\rm L}-\tilde\varepsilon_{\pm2}}\right|^2, \quad (12)$$

where the energies $\tilde\varepsilon_{\pm2}$ of the DE and $\tilde\varepsilon_0^{\rm U}$, $\tilde\varepsilon_{\pm1}^{\rm U,L}$ of the intermediate bright exciton states may differ from the unperturbed exciton energies ε_2 and $\varepsilon_0^{\rm U}$, $\varepsilon_1^{\rm U,L}$ (see Eq. (39) in Appendix A) by the energy of the phonons or dangling bond spin states participating in the transition as well as by the Zeeman energy of the excitons in an external magnetic field.

One can see that the dipole transition element $d_\perp^{\pm2}$ in Eq. (12) contains a superposition of the $V_{\rm e}$ and $V_{\rm h,1}$ perturbations. This is happening only because these perturbations result in the optical transitions between the same initial and final states of the NC. Generally, the dipole transition elements squared caused by the different perturbations are summarized. It is interesting to note, however, that the dipole $d_\perp^{\pm2}$ always contains a superposition of contributions of the lower, $\pm1^{\rm L}$, and the upper, $\pm1^{\rm U}$, intermediate exciton states. Straightforward calculation shows, that in the case when the energies of the DE and the intermediate bright exciton states coincide with the unperturbed exciton energies, when $\tilde\varepsilon_1^{\rm U,L}-\tilde\varepsilon_2 = \varepsilon_1^{\rm U,L}-\varepsilon_2 = \Delta/2+2\eta\pm\sqrt{f^2+d}$, the superposition is destructive for the $V_{\rm h,1}$ perturbation and Eq. (12) for the dipole transverse transition element squared is simplified into

$$|d_\perp^{\pm2}|^2 = |d_0|^2\frac{|V_{\rm e}|^2}{24\eta^2} \quad (13)$$

Below we consider interactions of excitons with an external magnetic field, phonons and dangling bond spins that result in non zero matrix elements $V_{\rm e}, V_{\rm h,1}$ and $V_{\rm h,2}$. The expressions for the ±2 DE transition matrix elements squared, $|d_\perp^{\pm2}|^2 = |d_0|^2\chi_\alpha^{21}$ and $|d_\parallel^{\pm2}|^2 = |d_0|^2\chi_\alpha^{20}$, induced by the coupling with $\pm1^{\rm U}$ and $0^{\rm U}$ bright excitons, respectively, via different coupling mechanisms α considered below, and the respective recombination rates $\Gamma_\alpha^{21} = 2\chi_\alpha^{21}/(R\tau_0)$ and $\Gamma_\alpha^{20} = \chi_\alpha^{20}/(\tau_0)$ are summarized in the Table I.

A. Activation by external magnetic field

In the case, when an external magnetic field $\boldsymbol{B} = (B_x, B_y, B_z)$ is applied to NCs, the perturbations terms are[11] $\hat V_{\rm e} = \frac{1}{2}g_{\rm e}\mu_{\rm B}(\boldsymbol{\sigma}^{\rm e}\boldsymbol{B})$ and $\hat V_{\rm h} = -g_{\rm h}\mu_{\rm B}(\boldsymbol{JB})$, where $g_{\rm e,h}$ are effective g-factors of the ground electron and hole states, respectively, $\mu_{\rm B}$ is the Bohr magneton.

The matrix elements $V_{\rm e} = g_{\rm e}\mu_{\rm B}(B_x - iB_y)/2$, $V_{\rm h,1} = -\sqrt{3}g_{\rm h}\mu_{\rm B}(B_x - iB_y)/2$ couples the ± 2 DE with $\pm 1^{\rm U,L}$ bright excitons resulting into $|d_\perp^{\pm 2}|^2$. Note, that matrix element $V_{\rm lh} = -g_{\rm h}\mu_{\rm B}(B_x - iB_y) \neq 0$ does not couple the ± 2 DE with any bright exciton state and $V_{\rm h,2} = 0$.

In addition to the coupling matrix elements, there are non zero diagonal matrix elements $V_{\uparrow,M} = (g_{\rm e}/2 - Mg_{\rm h})\mu_{\rm B}B\cos\theta$ and $V_{\downarrow,M} = -(g_{\rm e}/2 + Mg_{\rm h})\mu_{\rm B}B\cos\theta$, where θ is the angle between the magnetic field direction and the c-axis, which lead to the Zeeman splitting of the exciton states.[11,13] We assume, that the Zeeman energies $g_{\rm e}\mu_B B$ and $g_{\rm h}\mu_B B$ are much smaller than the energy separations between unperturbed exciton states $\varepsilon_1^{\rm L,U} - \varepsilon_2$, and neglect them in the denominator of Eq. (12). In this case, as it was shown above, the $V_{\rm h,1} \propto g_{\rm h}$ mediated coupling does not activate the dark exciton, because superposition of the $1^{\rm L}$ and $1^{\rm U}$ bright states results into the destructive contributions to the dipole transition element and thus to the radiative decay. In contrast, for $V_{\rm e} \propto g_{\rm e}$ mediated coupling the superposition of $1^{\rm L}$ and $1^{\rm U}$ bright states leads to constructive contributions to the dark exciton dipole transition element given by Eq. (13) and therefore to the PL, which is circularly polarized in the plane perpendicular to the c-axis. Substituting $|d_\perp^{\pm 2}|^2$ in Eq. (8) we obtain the rate of magnetic field assisted radiative recombination of the DE as $\Gamma_B = \Gamma_B^{21}$:[67]

$$\Gamma_B^{21} = \frac{|V_{\rm e}|^2}{12\eta^2}\frac{1}{R\tau_0} = \frac{[g_{\rm e}\mu_{\rm B}B\sin\theta]^2}{48\eta^2}\frac{1}{R\tau_0}\,, \qquad (14)$$

where $1/R = D_\perp/D_\parallel$ takes into account the anisotropy of the local field corrections to the probability of the optical transition in non spherical NCs. It is important to note that the rate of radiative recombination in Eq. (14) does not depend on the splitting between $\pm 1/2$ and $\pm 3/2$ hole states, Δ. Equation (14) shows also that the magnetic field activation of the DE becomes very efficient in large NCs, because $1/\eta^2 \sim a^6$.

The polarization properties of the magnetic field activated recombination from the ± 2 DE are the properties of the degenerate 2D dipole determined by coupling with the $\pm 1^{\rm L,U}$ bright excitons. The activation process is shown schematically in Fig. 2(a). The resulting PL is directed preferably along the c-axis and circularly polarized in the plain perpendicular to the c-axis. Introduced in the previous section, the polarization anisotropy parameter for the magnetic field activation of the DE is $r_{\rm d}^B = Rf_{\rm d}^B = 0$.

B. Phonon assisted recombination of the ± 2 DE

Let us consider phonon assisted radiative recombination of the ± 2 DE. In spherical NCs, each long-wave length acoustic and optical phonon is characterized by total angular momentum l and its projection m on the quantization axis. The wave functions of corresponding

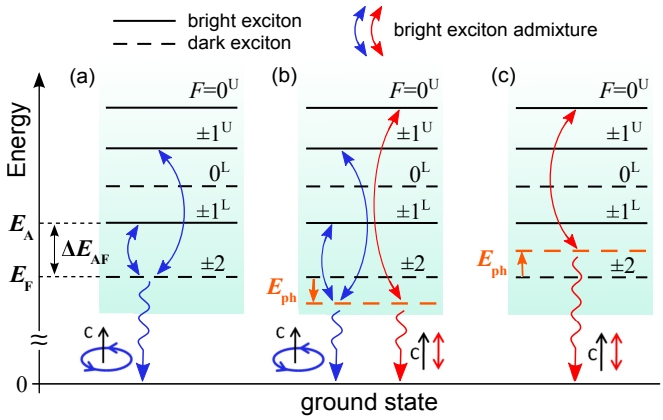

FIG. 2: Schematic image of the fine structure of the band edge exciton and the radiative decay of the ± 2 dark exciton activated by the external magnetic field or dangling bond spins (a) and phonon assisted transitions (b) and (c). Bright and dark exciton levels are shown by solid and dashed lines, respectively. The solid arrows show the optically active levels that admix to the DE via different activation mechanism. The vertical waving arrows show the energy of emitting photons. The PL polarization of the DE decay is controlled by the dipoles of optically active levels to which the DE is admixed and corresponding polarizations are show by the circle arrow around the NC c-axis and by the arrow parallel to the c-axis. The phonon assisted Stokes lines red shifted by the phonon energy, $E_{\rm ph} = E_{\rm LO}$ in (b), could have polarization properties of the $\pm 1^{\rm L,U}$ (shown in blue) and the $0^{\rm U}$ (shown in red) bright excitons, respectively. The Stokes (b) and anti-Stokes (c) acoustic phonon activated line with $E_{\rm ph} = E_{\rm AC}$ has polarization properties only of the $0^{\rm U}$ exciton.

spherical optical and acoustic phonons where introduced in Refs.68,69 and Refs.70,71, and Hamiltonians that describe their interaction with electrons and holes have been derived in Refs.56,72 and Refs. 58,71,73, respectively. The interaction of the carriers with the spherical phonons always has a form of expansion over the full system of eigen-functions of the orbital momentum operator $\sum_l C_l^{\rm ph}(a_{lm}Y_{lm} + a_{lm}^\dagger Y_{lm}^*)$, where Y_{lm} are the spherical harmonics, the operators a_{lm} and $a_{lm}^\dagger$ are the operators of creation and annihilation of the phonons with energy $E_{\rm ph}$, total angular momentum l and projection m, and the coefficients $C_l^{\rm ph}$ depend on the NC size, type of participating phonons, and interaction mechanism.[56,58,71–73]

Coupling of phonons with the ground $1S$ electron, does not activate the radiative recombination of the ± 2 DE because $V_{\rm e} = 0$. The interactions of phonons with holes, however, result in the hole-momentum flip assisted recombination of the DE. It was demonstrated,[74] that only terms proportional to $Y_{2,\pm 2}$ and $Y_{2,\pm 1}$ couple the wave functions of the hole ground state, Ψ_M, with initial and final hole momentum projections, M, differing by ± 1 or ± 2. These terms result in nonvanishing matrix elements $|V_{\rm h,2}| = |C_2^{\rm ph}\langle\Psi_{\pm 3/2}|Y_{2\mp 2}|\Psi_{\mp 1/2}\rangle| = V_{\rm ph}$ and $|V_{\rm h,1}| = |C_2^{\rm ph}\langle\Psi_{\pm 3/2}|Y_{2\pm 1}|\Psi_{\pm 1/2}\rangle| = V_{\rm ph}$.

Generally, the phonon assisted radiative decay of the DE shifts the energy of emitted photons by the energy of a phonon participating in optical transitions, $E_{\rm ph}$. The matrix element $V_{\rm h,1}$ couples the DE with the $\pm 1^{\rm L,U}$ bright excitons. In the case $\tilde{\varepsilon}_1^{\rm U,L} - \tilde{\varepsilon}_2 = \varepsilon_1^{\rm U,L} - \varepsilon_2 \pm E_{\rm ph}$, and the destructive superposition of the contributions from the $\pm 1^{\rm L,U}$ states does not eliminate the transverse dipole transition element $d_\perp^{\pm 2}$ of Eq. (12). The phonon assisted recombination of the DE contributes to the two PL lines with energies $\hbar\omega = E_{\rm F} \mp E_{\rm ph}$. The rate of their recombination calculated in the second order perturbation theory is described, correspondingly, as

$$\Gamma_{\rm ph}^{21}(E_{\rm F} \mp E_{ph}) = \frac{V_{\rm ph}^2 E_{\rm ph}^2 (N_{\rm B} + 1/2 \pm 1/2)}{4(3\Delta\eta \pm E_{\rm ph}(\Delta + 4\eta) + E_{\rm ph}^2)^2} \frac{1}{R\tau_0} \,. \tag{15}$$

Here $N_{\rm B}(E_{\rm ph}, T) = [\exp(E_{\rm ph}/kT) - 1]^{-1}$ is the Boltzmann population function (k - is the Boltzmann constant) for the phonons participating in recombination, which depends on their energy, $E_{\rm ph}$, and temperature, T. The $V_{\rm h,2}$ interaction mediates DE coupling with the $0^{\rm U}$ bright exciton state. As a result, the DE acquires a dipole $d_\parallel^{\pm 2}$, given by Eq. (11) with denominator $\tilde{\varepsilon}_0^{\rm U} - \tilde{\varepsilon}_{\pm 2} = \varepsilon_0^{\rm U} - \varepsilon_{\pm 2} \pm E_{\rm ph}$. In this case, the phonon assited recombination of the DE occurs at the frequencies $\hbar\omega = E_{\rm F} \mp E_{\rm ph}$ with the rates

$$\Gamma_{\rm ph}^{20}(E_{\rm F} \mp E_{\rm ph}) = \frac{V_{\rm ph}^2 (N_{\rm B} + 1/2 \pm 1/2)}{2(\Delta + 4\eta \pm E_{\rm ph})^2} \frac{1}{\tau_0} \,. \tag{16}$$

The typical energy of the acoustic phonons $E_{\rm ph} = E_{\rm AC}$ is much smaller than $\Delta E_{\rm AF}$. This suppresses the phonon assisted recombination described by Eq. (15) because $E_{\rm AC}^2/(3\eta\Delta) \leq (E_{\rm AC}/\Delta E_{\rm AF})^2 \ll 1$. As a result, the acoustic phonon-assisted recombination of the DE is dominated by transitions described in Eq. (16) and have polarization properties of the $0^{\rm U}$ bright exciton, which is linearly polarized along c-axis (see red arrows in Figs. 2b and 2c). Emission or absorption of the phonons with energy $E_{\rm ph} = E_{\rm AC}$ result in Stokes and anti-Stokes lines shifted down and up from $E_{\rm F}$ by the acoustic phonon energy $E_{\rm AC}$, respectively. The intensities of these components are proportional to $N_{\rm B} + 1$ and $N_{\rm B}$, correspondingly. At low temperatures that are smaller than the acoustic phonon energy, ($kT \ll E_{\rm AC}$), only the Stokes component is expected. However, even a slight increase in temperature can activate the DE recombination assisted by the acoustic phonons. Neglecting a weak dependence of $\Gamma_{\rm ph}^{20}(E_{\rm F} \mp E_{\rm ph})$ on the acoustic phonon energy $E_{\rm ph} = E_{\rm AC} \ll \Delta$, one can write the total rate of the acoustic-phonon assisted recombination as

$$\Gamma_{\rm AC} = \Gamma_{\rm AC}^{20} = \frac{V_{\rm ph}^2}{(\Delta + 4\eta)^2} \frac{\coth(E_{\rm AC}/2kT)}{2\tau_0} \,. \tag{17}$$

In the FLN experiments, the Stokes and anti-Stokes lines are not resolved separately and both contribute to a ZPL. As a result of these line contributions, the temperature increase leads to a blue shift of the ZPL described as $E_{\rm F} - E_{\rm AC} \tanh(E_{\rm AC}/2kT)$. The intensity of the PL increases with temperature as $\coth(E_{\rm AC}/2kT)$.

In the case of the optical-phonon assisted recombination, the phonon energy $E_{\rm ph} = E_{\rm LO}$ can not be neglected in Eqs. (16) and (15), because it is comparable or even larger than $\Delta E_{\rm AF}$. In the range of temperatures we consider here, $kT \ll E_{\rm LO}$, only Stokes PL line with energy $\hbar\omega = E_{\rm F} - E_{\rm LO}$, can be observed. The LO phonon assisted radiative decay rate of the DE is almost temperature independent and given by

$$\Gamma_{\rm LO} = \Gamma_{\rm ph}^{20}(E_{\rm F} - E_{\rm LO}) + \Gamma_{\rm ph}^{21}(E_{\rm F} - E_{\rm LO}). \tag{18}$$

Here the rates $\Gamma_{\rm ph}^{20}$ and $\Gamma_{\rm ph}^{21}$ are described by Eqs. (16) and (15) with $E_{\rm ph} = E_{\rm LO}$ and $N_{\rm B} \approx 1$.

The polarization of the acoustic phonon assisted recombination of the DE is determined by the non degenerate 1D dipole of the $0^{\rm U}$ bright exciton. The activation processes of the DE via $\pm 0^{\rm U}$ bright exciton are shown schematically by red arrows in Figs. 2(b) and (c) for the Stokes and anti Stokes components, respectively. The resulting PL of the DE, which is directed preferably perpendicularly to the c- axis of the NC, is liner polarized along c-axis. The polarization anisotropy parameter is $r_{\rm d}^{\rm AC} = Rf_{\rm d}^{\rm AC} \to \infty$.

The polarization of the optical phonons assisted emission of the DE is mixed due optical phonon coupling with the $0^{\rm U}$ bright exciton characterized by the nondegenerate 1D dipole and with the $\pm 1^{\rm L,U}$ bright excitons characterized by the degenerate 2D dipole. The activation process via $\pm 1^{\rm L,U}$ bright excitons is shown schematically by blue arrows in Fig. 2(b) for the Stokes component. The resulting PL directed preferably along the NC c- axis is circularly polarized in the plain perpendicular to the c-axis. The polarization anisotropy parameter for the optical phonon assisted mechanism can be found as

$$\begin{aligned} r_{\rm d}^{\rm LO} &= Rf_{\rm d}^{\rm LO} = R\frac{|d_\parallel^{\pm 2}|^2}{|d_\perp^{\pm 2}|^2} \\ &= R\frac{4[3\Delta\eta + E_{\rm LO}(\Delta + 4\eta) + E_{\rm LO}^2]^2}{E_{\rm LO}^2[\Delta + 4\eta + E_{\rm LO}]^2} \,. \end{aligned} \tag{19}$$

One can see, that for $\Delta > 0$ and $R \approx 1$, the parameter $r_{\rm d}^{\rm LO}$ is always lager than 4. As a result, the optical phonon assisted line of the DE PL in nearly spherical NCs made of wurtzite CdSe is mostly linear polarized along c-axis of the NC.[48,49]

C. Dangling bond assisted recombination of the ± 2 DE

The dangling bond assisted mechanism of the ± 2 DE radiative recombination was suggested recently in Ref. [45]. Indeed an exchange interaction between the exciton spin and the spins of the dangling bonds at the NC surface could result in flip-flop processes, which mix up the ± 2 DE with the $\pm 1^{\rm L,U}$ bright excitons. Flipping the

dangling bond spins could change the exciton spin projection by ± 1. The exchange interaction between the dangling bond spins and the exciton spins is dominated by their interaction with the electron spins, because an electron wave function more strongly penetrates to the NC surface. Here we assume that the NC have a spherical shape and the exchange interaction of an electron in the ground $1S_{\rm e}$ state with all dangling bonds is the same and can be characterized by the one exchange constant α (see details in Ref. [45]). As a result the electron-dangling bond spin exchange interaction can be written as:

$$\hat{H}_{\rm ss} = -\alpha \sum_j \hat{\boldsymbol{\sigma}}^{\rm e} \hat{\boldsymbol{\sigma}}^j, \tag{20}$$

where $\hat{\boldsymbol{\sigma}}^{\rm e}$ and $\hat{\boldsymbol{\sigma}}^j$ are the Pauli matrixes for the electron and j-th dangling bond spins, correspondingly. Each j-term in the sum of the exchange Hamiltonian of Eq. (20) could provide the simultaneous spin flip-flop of the electron spin projection and the projection of j-th dangling bond spin described by the matrix element $|V_{\rm e}| = 2\alpha$. Consequently, the $V_{\rm e}$ mediated coupling with $\pm 1^{\rm L,U}$ bright excitons results into the transverse dipole transition element given by Eq. (13). The sum over all dangling bond spins results in

$$|d_{\perp}^{\pm 2}|^2 = |d_0|^2 \frac{\alpha^2}{6\eta^2} N_{\rm db}^{\mp}, \tag{21}$$

where $N_{\rm db}^{+}$ and $N_{\rm db}^{-}$ are the numbers of dangling bond spins oriented along and opposite to the c-axis, respectively.

The random fluctuation of the dangling bond spins orientation results in the dangling bond spin polarization along the NC c-axis

$$\rho_{\rm db} = -\frac{\sum_j \langle \hat{\sigma}_z^j \rangle}{N_{\rm db}} = \frac{N_{\rm db}^{-} - N_{\rm db}^{+}}{N_{\rm db}}. \tag{22}$$

Here $N_{\rm db} = N_{\rm db}^{-} + N_{\rm db}^{+}$ is the total number of dangling bonds at the NC surface. The dangling bond polarization split the ± 2 DE into two spin sub-levels. The splitting is proportional to the dangling bond spin polarization $\Delta E_{\rm ex} = 2\alpha N_{\rm db} \rho_{\rm db}$. This splitting in turn results in a different relative population of the exciton spin sublevels $N_{{\rm ex},\pm 2}$, which also have different dangling bond assisted recombination rates. Straightforward calculations in second order perturbation theory which takes the last effect into account gives the following rate for the dangling bond assisted radiative recombination as $\Gamma_{\rm db} = \Gamma_{\rm db}^{21}$:[45]

$$\Gamma_{\rm db}^{21} = \gamma_{\rm ex} N_{\rm db} \left[1 - \rho_{\rm db} \rho_{\rm ex}\right], \tag{23}$$

where $\gamma_{\rm ex} = [(\alpha/\eta)^2/(6R\tau_0)]$ is the electron-dangling bond spin-flip rate, $\rho_{\rm ex} = (N_{{\rm ex},-2} - N_{{\rm ex},+2})/N_{\rm ex} = \tanh[\alpha N_{\rm db}\rho_{\rm db}/kT]$ is the polarization of the exciton state, and $N_{\rm ex}$ is the averaged number of excitons per NC.

At high temperatures, when dangling bonds are not polarized and randomly oriented ($N_{\rm db}^{-} = N_{\rm db}^{+} = N_{\rm db}/2$), the dangling bond assisted DE recombination rate is just proportional to the total number of dangling bonds: $\Gamma_{\rm db} = \gamma_{\rm ex} N_{\rm db}$. As we have shown in Ref. 45, the radiative recombination is suppressed at low temperatures, when $\rho_{\rm db}\rho_{\rm ex} \longrightarrow 1$ due to the formation of the dangling bond magnetic polaron state.

The polarization properties of the dangling bond assisted recombination from the DE are determined by the coupling with the $\pm 1^{\rm L,U}$ bright excitons and the 2D dipole acquired by the DE is oriented transverse to the c-axis. The activation process is shown schematically in Fig. 2(a). The resulting PL is directed preferably along the c-axis and circularly polarized in the plane perpendicular the c-axis. The polarization anisotropy parameter for the dangling bond spin flip–assisted recombination of the ± 2 DE is the same as for the external magnetic field activation: $r_{\rm d}^{\rm db} = R f_{\rm d}^{\rm db} = 0$.

IV. MAGNETIC FIELD ASSISTED RADIATIVE RECOMBINATION OF THE $\mathcal{F} = 2$ DARK EXCITON IN SPHERICAL OR "QUASI-SPHERICAL" NCS

In spherical or "quasi-spherical" NCs with $\Delta = 0$ the ground exciton state is a five fold degenerate DE with total angular momentum $\mathcal{F} = 2$. In this case, all states are characterized by their projections on the direction of an external magnetic field $\boldsymbol{B}$. The states can be still notated as ± 2, $\pm 1^{\rm L}$ and $0^{\rm L}$ for the dark exciton and $\pm 1^{\rm U}$ and $0^{\rm U}$ for the upper bright exciton with $\mathcal{F} = 1$. In this case the magnetic field does not mix up the states with different momentum projections and, at first glance, does not activate the ground DE. Surprisingly, however, it activates the DE via a magnetic field induced coupling between dark ($\mathcal{F} = 2$) and bright ($\mathcal{F} = 1$) exciton states with the same momentum projections on the $\boldsymbol{B}$ direction.

The magnetic field stimulated coupling of $0^{\rm L}$ and $\pm 1^{\rm L}$ DEs with $0^{\rm U}$ and $\pm 1^{\rm U}$ bright excitons, are described by the following matrix elements:

$$\langle \pm 1^{\rm U} | \hat{V}_{\rm e} + \hat{V}_{\rm h} | \pm 1^{\rm L} \rangle = \frac{\sqrt{3}}{2} \langle 0^{\rm U} | \hat{V}_{\rm e} + \hat{V}_{\rm h} | 0^{\rm L} \rangle = \frac{\sqrt{3}}{4} \mu_{\rm B} (g_{\rm e} + g_{\rm h}) B. \tag{24}$$

The resulting radiative rates are given by

$$\Gamma_B^{11} = \frac{3}{4R} \Gamma_B^{00} = \frac{3}{R\tau_0} \frac{[\mu_{\rm B}(g_{\rm e} + g_{\rm h})B]^2}{256\eta^2}. \tag{25}$$

We assume again that all Zeeman energies are much smaller than the exchange splitting 4η.

The five sublevels of the $\mathcal{F} = 2$ exciton are split in a magnetic field as $E_F = g_{\rm ex}\mu_{\rm B} B F$ with the DE g factor $g_{\rm ex} = (g_{\rm e} - 3g_{\rm h})/4$. This value is positive in CdSe

Coupling to	$\pm1^{\rm L,U}$ states	Coupling to $0^{\rm U}$ state
Polarization	$\perp$ $\boldsymbol{c}$-axis	$\parallel$ $\boldsymbol{c}$-axis
Dipole element	$\lvert d_\perp\rvert^2 = \lvert d_0\rvert^2 \cdot \chi_\alpha^{01}$	$\lvert d_\parallel\rvert^2 = \lvert d_0\rvert^2 \cdot \chi_\alpha^{00}$
Radiative rate	$\Gamma_\alpha^{01} = \dfrac{2}{R}\dfrac{1}{\tau_0} \cdot \chi_\alpha^{01}$	$\Gamma_\alpha^{00} = \dfrac{1}{\tau_0} \cdot \chi_\alpha^{00}$
Mechanism (α)	χ_α^{01}	χ_α^{00}
Magnetic field (B)	$[g_{\rm e} - 2g_{\rm h}]^2 \dfrac{[\mu_{\rm B} B \sin\Theta]^2}{32\eta^2}$	$[g_{\rm e} + g_{\rm h}]^2 \dfrac{[\mu_{\rm B} B \cos\Theta]^2}{64\eta^2}$
Dangling bonds (db)	$\dfrac{\alpha^2}{4\eta^2} N_{\rm db}$	$\dfrac{\alpha^2}{16\eta^2}\left[N_{\rm db}(N_{\rm db}-1)\rho_{\rm db}^2 + N_{\rm db}\right]$
Acoustical phonons (AC)	$\dfrac{3V_{\rm AC}^2 E_{\rm AC}^2}{8[(-\Delta\eta + E_{\rm AC}^2)^2 - (-\Delta+4\eta)^2 E_{\rm AC}^2)]^2} \times \left[(-\Delta\eta + E_{\rm AC}^2)\coth\dfrac{E_{\rm AC}}{2kT} - (-\Delta+4\eta)E_{\rm AC}\right]$	
Optical phonons (LO)	$\dfrac{3V_{\rm LO}^2 E_{\rm LO}^2}{8(-\Delta\eta + E_{\rm LO}(-\Delta+4\eta) + E_{\rm LO}^2)^2}$	

TABLE II: Radiative decay rates and polarization properties of the $0^{\rm L}$ DE activated by various physical mechanisms. For activation caused by magnetic field (B), dangling bonds (db), acoustic (AC) and optical (LO) phonons, the squares of the dipole transition matrix elements, $|d_\perp^{\pm2}|^2 = |d_0|^2\chi_\alpha^{21}$ and $|d_\parallel^{\pm2}|^2 = |d_0|^2\chi_\alpha^{20}$, induced by the coupling of the ±2 DE with $\pm1^{\rm U}$ and $0^{\rm U}$ bright excitons, respectively, where $\alpha = B, {\rm db}, {\rm AC}$ and LO. The radiative recombination rates induced by these activation mechanisms can be written correspondingly $\Gamma_\alpha^{21} = 2\chi_\alpha^{21}/(R\tau_0)$ and $\Gamma_\alpha^{20} = \chi_\alpha^{20}/(\tau_0)$.

NCs, and as a result the lowest DE state has spin projection $F = -2$, which is not activated by the longitudinal magnetic field. The resulting rates of the radiative recombination from the $\mathcal{F} = 2$ DE and its polarization is determined by the relative populations of the Zeeman sublevels given by $N_F = \exp(-E_F/kT)/N_{\rm ex}$, where $N_{\rm ex} = \sum_{F=0,\pm1,\pm2}\exp(-E_F/kT)$. The total radiative rate of the DE in an external magnetic field can be written as

$$\Gamma_B = (\Gamma^0 + \Gamma_B^{00})N_0 \; + \; (\Gamma^1 + \Gamma_B^{11})[N_{-1} + N_{+1}] \; + \; \Gamma^2[N_{-2} + N_{+2}]\,, \qquad (26)$$

where Γ^0, Γ^1 and Γ^2 are the radiative rates of the DE sublevels with projections 0, ±1 and ±2 on the magnetic field directions, respectively, that are coursed by other than the external magnetic field activation mechanisms. One can see, that Γ_B from Eq. (26) is a non-monotonic function of the magnetic field.

V. RADIATIVE RECOMBINATION OF THE $0^{\rm L}$ DARK EXCITON

We turn now to the radiative decay rate of the $0^{\rm L}$ ground state DE activated by different physical mechanisms which mix it with the bright excitons. The matrix representation of the exciton hamiltonian in Eq. (2) shows clearly that $V_{\rm e}$, $V_{\rm lh}$ and $V_{\rm h,1}$ terms couple the $0^{\rm L}$ DE with $\pm1^{\rm L,U}$ bright excitons, while $V_{\rm h,2}$ does not help in the DE activation. In addition, diagonal matrix elements $V_{\uparrow,-1/2}$ and $V_{\downarrow,1/2}$ also couple $0^{\rm L}$ DEs with $0^{\rm U}$ bright excitons. Calculations of the radiative decay rate are similar to those done for the ±2 DE. The details of the calculations can be found in the Appendix B. The expressions for the $0^{\rm L}$ DE transition matrix elements squared, $|d_\perp^{\pm2}|^2 = |d_0|^2\chi_\alpha^{01}$ and $|d_\parallel^{\pm2}|^2 = |d_0|^2\chi_\alpha^{00}$, induced by the coupling with $\pm1^{\rm U}$ and $0^{\rm U}$ bright excitons, respectively, via different coupling mechanisms α, and the respective recombination rates $\Gamma_\alpha^{01} = 2\chi_\alpha^{01}/(R\tau_0)$ and $\Gamma_\alpha^{00} = \chi_\alpha^{20}/(\tau_0)$ are summarized in the Table II. The respective activation processes and their polarization are shown schematically in Fig. 3.

It is important to note that contrary to the case of the ±2 DE, the activation of the $0^{\rm L}$ DE by an external magnetic field and the dangling bond spin flip–assisted mechanism results in PL which have different polarization properties. The coupling of the $0^{\rm L}$ DE with the $0^{\rm U}$, $+1^{\rm U,L}$ and $1^{\rm U,L}$ bright excitons by the magnetic field leads to a coherent superposition of these three intermediate states, contributing to the PL in the second order perturbation theory. The straightforward calcula-

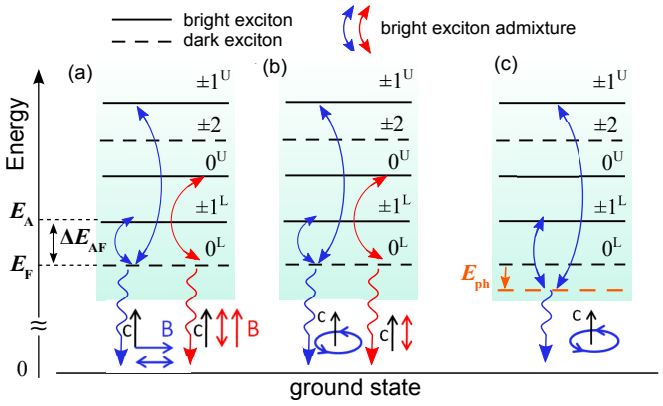

FIG. 3: Schematic image of the fine structure of the band edge exciton and the radiative decay of the dark 0^L exciton activated by the external magnetic field (a) dangling bond spins (b) and phonon assisted transition (c). Bright and DE levels are shown by solid and dashed lines, respectively. The solid arrows show the optically active levels that admix to the DE via different activation mechanisms. The vertical waving arrows show the energy of emitting photons. The PL polarization of the DE decay is controlled by the dipoles of optically active levels to which the dark exciton is admixed and corresponding polarizations are show by the circle arrow around the NC c-axis and by the arrow perpendicular or parallel to the c-axis. For the phonon assisted transition only Stokes lines red shifted by the phonon energy, $E_{\rm ph} = E_{\rm LO}$ or $E_{\rm ph} = E_{\rm AC}$, is shown on (c).

tions show that this superposition results in a linearly polarized PL. The activation of 0^L DE by a magnetic field either parallel or perpendicular to the c-axis results in PL linearly polarized parallel to the magnetic field. In contrast, the dangling bond spins activation results in PL with mixed polarization properties: PL linear polarized along the c-axis of the NC and PL circularly polarized around its c-axis. The detailed explanations for these properties are given in the Appendix B.

VI. DISCUSSION

Let us first discuss how our theory of the DE activation describes the PL properties of most heavily studied CdSe NCs where the ±2 DE is the ground exciton level. The optical phonon assisted radiative recombination of the DE clearly seen in FLN experiments[20] is a direct proof that the exciton coupling with the optical phonon courses such an activation. The PL lines related to the acoustic phonon assisted recombination of the DE are not resolved usually in FLN experiments because an inhomogeneous broadening of the ZPL is much larger than the energies of NC acoustic phonons. They have been observed, however, in the SD experiments[27,31] and in the FLN spectra of the CdSe/CdS dot-in-rod heteronanocrystals[25] due to the much narrower ZPL linewidth. In the CdSe/CdS dot-in-rod NCs the electron wave function is strongly anisotropic due to its leakage to the CdS shell. This anisotropy leads to an additional phonon-assisted recombination mechanism of the DE, which was not considered in our paper.

Experimentally, the rate of the DE recombination in zero magnetic field is usually determined from the temperature dependence of the PL life time long component, $\tau_{\rm L}$.[27,33,34,36] In this model the DE recombination rate $\Gamma_{\rm F} \equiv \Gamma_{\rm DE}$ is assumed to be temperature independent, and the temperature dependence of $\tau_{\rm L}$ is determined solely by the temperature induced population of the bright exciton state with the recombination rate $\Gamma_{\rm A} \gg \Gamma_{\rm F}$ according to:[34]

$$\frac{1}{\tau_{\rm L}} = \Gamma_{\rm F}\frac{1}{1+\exp\left(-\Delta_{\rm AF}/kT\right)} + \Gamma_{\rm A}\frac{\exp\left(-\Delta_{\rm AF}/kT\right)}{1+\exp\left(-\Delta_{\rm AF}/kT\right)}\,. \tag{27}$$

Here $\Delta_{\rm AF}$ is the bright–dark exciton splitting, which is usually obtained by fitting of the experimentally measured temperature dependence of $\tau_{\rm L}$. Measured in NCs with different sizes, the procedure gives a size dependence of $\Delta_{\rm AF}$, which sometimes resembles a more size dependence of confined acoustic phonons than the size dependence of the splitting between dark and bright excitons.[36,37] It is important to note, however, that some of the DE activation mechanisms considered above predict the temperature dependence of $\Gamma_{\rm F}$ itself.

First of all, the DE radiative recombination rate assisted by acoustic phonons increases with temperature as $\coth(E_{\rm AC}/2kT)$, in the range where this rate is still smaller than the bright exciton radiative recombination rate. Second, the dangling bond spin assisted radiative recombination of the DE becomes temperature dependent in small NCs due to formation and thermal dissociation of the magnetic polaron.[45] Therefore, the mechanism of the dangling bond spin assisted recombination suggests the existence of additional activation energies for $\tau_{\rm L}$ at temperatures below the bright exciton activation.

Other important consequences of different activation mechanisms are the different polarization properties of the DE recombination. We have shown that the dangling bond spin flip–assisted recombination of the ±2 DE is the only activation mechanism which results in the PL polarization described by the degenerate 2D dipole in zero magnetic field. Only for this mechanism, the anisotropy parameter of the DE recombination is the same as for the lowest bright exciton: $r_{\rm d}^{\rm db} = Rf_{\rm d}^{\rm db} = R|d_{\parallel}^{\pm2}|^2/|d_{\perp}^{\pm2}|^2 = 0$. The DE activation via the acoustic phonons lead to $r_{\rm d}^{\rm AC} = Rf_{\rm d}^{\rm AC} \to \infty$. For the DE activation by optical phonons $r_{\rm d}^{\rm LO} = Rf_{\rm d}^{\rm LO} > 4$ for $R \geq 1$. Therefore, we conclude that the dangling bond spin flip–assisted mechanism is responsible for DE radiative recombination in single CdSe NCs with diameter 5.2 nm and 3.8 nm studied in Ref. [50]. These NCs have demonstrated the polarization properties of the degenerate 2D dipole at the temperature 10K.

On the other hand, the dangling bond spin flip-assisted

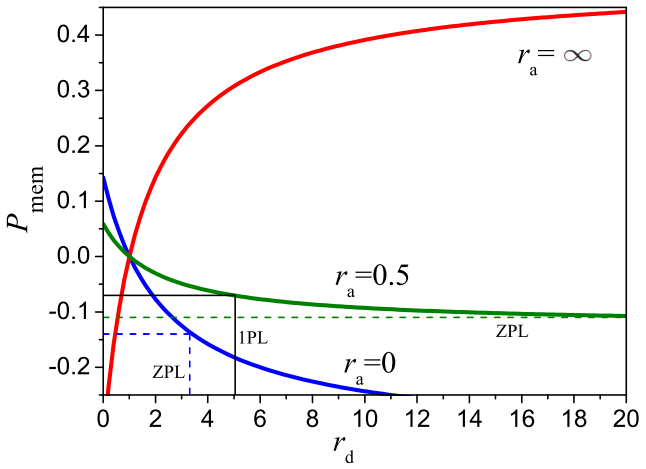

FIG. 4: Dependencies of the linear polarization memory degree $P_{\rm mem}$ on the anisotropy parameter $r_{\rm d}$. The blue line describes the $P_{\rm mem}$ dependence in the case resonant excitation of the ± 1 bright excitons for which $r_{\rm a} = 0$. The red line describes the $P_{\rm mem}$ dependence in the case of resonant excitation of the $0^{\rm U}$ bright excitons for which $r_{\rm a} = \infty$. The green line describes the mixed excitation condition for which $r_{\rm a} = 0.5$. Horizontal lines show the experimentally observed values of the polarization memory degree. The blue dashed horizontal line corresponds to the value -0.14 observed in Ref. 21 for ZPL at T=10K after the resonant excitation with $r_{\rm a} = 0$ and relaxation into the DE state. The green dashed and black solid horizontal lines correspond to the values -0.11 and -0.07 observed in Ref. 12 for ZPL and 1PL, respectively, at T=2K.

recombination might be suppressed at low temperatures in small NCs.[45] In this case, the main mechanism responsible for the ZPL seen in the FLN experiments, is acoustic phonon assisted recombination of the DE. This recombination leads to the PL which is linearly polarized along c-axis. This prediction allows us to explain the experimental observations of the negative linear polarization memory in CdSe NCs reported in Refs. 12,21. In Ref. 21 the PL was excited resonantly by linear polarized light. At the initial period just after the excitation, the PL was co-polarized to the excitation with the positive linear polarization degree $P_{\rm mem} \approx 0.143$.[75] This number is in a very good agreement with theoretically predicted polarization memory degree $1/7 \approx 0.143$ for the resonance excitation of the lowest $\pm 1^{\rm L}$ bright exciton and emission from the same excited state.[48] At low temperatures (below 10 K), the polarization changed its sign after some small time delay, and the ZPL PL became cross-polarized to the excitation with the negative polarization memory $P_{\rm mem} \approx -0.14$. The time dependence of the degree of the PL polarization is identical to those of the PL[21], what confirms the change of the emitting state after the exciton relaxation to the ground DE state. Therefore, the observed negative polarization memory is determined by the DE activation mechanism. Generally, the degree of PL polarization memory in an ensemble of randomly oriented NCs is given by:[48]

$$P_{\rm mem} = \frac{I_\parallel - I_\perp}{I_\parallel + I_\perp} = \frac{(r_{\rm a}-1)(r_{\rm d}-1)}{7 + 3r_{\rm d} + r_{\rm a}(3+2r_{\rm d})}\,, \qquad (28)$$

where $I_\parallel$ ($I_\perp$) are intensity of the PL polarized parallel (perpendicular) to the polarization of exciting light, and $r_{\rm a} = Rf_{\rm a} = Rd_\parallel|^2/|d_\perp|^2$ characterizes the anisotropy of selection rules for the bright excitons. For the resonance excitation of the $\pm 1^{\rm L,U}$ bright excitons $r_{\rm a} = 0$ and of the $0^{\rm U}$ bright exciton $r_{\rm a} = \infty$. The dependence of the linear polarization memory degree $P_{\rm mem}$ on the anisotropy parameter $r_{\rm d}$ for the resonant excitation of the ± 1 and $0^{\rm U}$ bright excitons are shown in Fig. 4 by the blue and red lines, respectively. The horizontal and vertical dashed blue lines show the experimentally observed in Ref. 21 at 10K value of $P_{\rm mem} \approx -0.14$ and the corresponding $r_{\rm d} \approx 3.41$, respectively. This value of the $r_{\rm d}$ indicates that the dangling bond assisted mechanism is partially suppressed at 10K. However, increasing the temperature to 20-30K decreases the degree of linear polarization suggesting the activation of the dangling bond assisted recombination.[21] The temperature dependent Stokes shift of the ZPL observed in Ref.21 also confirms the magnetic polaron formation in these NCs at low temperatures and its dissociation with temperature increase. Note, that in the case of the complete suppression of the dangling bond spin assisted mechanism $r_{\rm d} \to \infty$ and Eq. (28) predicts $P_{\rm mem} \to -0.33$ for the resonant excitation with $r_{\rm a} = 0$.

The effect of the negative polarization memory was reported also in CdSe nanocrystals embedded in a glass matrix.[12,22] In Ref. 12, the excitation was not in exact resonance with the lowest $\pm 1^{\rm L}$ bright exciton and some fraction of the NCs were excited at the level of $0^{\rm U}$ bright exciton. This was evidenced, for example, from the large positive polarization memory degree up to 0.3 just after the excitation. Equation (28) and the red curve in Fig. 4 show that in the case when both the excitation and detection are characterized by $r_{\rm a} = r_{\rm d} \to \infty$, the $P_{\rm mem}$ maximum reaches 0.5. After $\sim$ 100 ps delay, the negative polarization memory was observed for both ZPL and in the optical phonon assisted lines. The negative polarization memory degree of -0.11 and -0.07, measured for the ZPL and 1PL under steady state excitation conditions[12] are shown in Fig. 4 by the horizontal green dashed and black solid lines, respectively. The green line shows the dependence of $P_{\rm mem}$ on $r_{\rm d}$ calculated for a resonant excitation characterized by $r_{\rm a} = 0.5$. One can see that the observed degrees of polarization memory are in a good agreement with the theoretical expectations: $r_{\rm d} \geq 4$ for the 1PL and $r_{\rm d} \gg 1$ for the ZPL. These calculations show that the acoustic phonon assisted recombination is the main mechanism of the DE radiative decay responsible for the ZPL in CdSe NCs embedded in a glass matrix.

Thus, the measurement of the linear polarization memory effect at low temperatures can reveal the exciton fine structure and the activation mechanisms of the lowest ± 2 DE responsible for its radiative decay. Gener-

ally, the anisotropy polarization parameter of emission $f_{\rm d} = |d_{\|}|^2/|d_{\perp}|^2$ and consequently $r_{\rm d} = Rf_{\rm d}$ may depend on the temperature due to temperature dependence of some of the activation mechanisms. This parameter also depends on the external magnetic field[49] due to field induced activation of the DE. In time–resolved experiments this parameter may change with time due to an exciton thermalization to the lower lying exciton levels after the excitation. Therefore, the theory predicts strong changes in the polarization of emitted light with time or with increase of the temperature or an external magnetic field.

For the spherical or "quasi-spherical" NCs with $\Delta = 0$, where the lowest degenerate DE is characterized by the total momentum $\mathcal{F} = 2$, we have considered the activation of this state by an external magnetic field. It is usually assumed that the activation of the DE and the shortening of the DE life time in external magnetic field in NC made from cubic semiconductors is a signature of the NC shape anisotropy.[39,41] We have demonstrated, however, that the magnetic field can activate the DE in spherical cubic NCs and the dependence of the DE lifetime on the magnetic field might be non monotonic.

We have demonstrated that the $0^{\rm L}$ DE can be activated by the external magnetic field, acoustic and optical phonons and dangling bond spins. Experimentally, the lowest $0^{\rm L}$ DE was studied using SD experiments in prolate CdSe NC.[76,77] In these studies, the PL from the $0^{\rm L}$ DE was observed only in the presence of an external magnetic field and without the field was not detected neither in the PL nor in the PLE measurements. The absence of the PL from the $0^{\rm L}$ exciton without a magnetic field does not have a clear explanation. In all NCs studied with the lowest $0^{\rm L}$ DE, the bright–dark splitting is very small, of the order of 0.5 meV, and the bright $\pm 1^{\rm L}$ exciton remains well populated even at 2 K. The state selective pumping experiments[77] conducted in these NCs show that the exciton relaxation to the ground exciton state is suppressed and the state population distributions depend significantly on the pumping conditions. This suggests that the absence of the PL from the $0^{\rm L}$ DE in zero magnetic field might be connected with its low population. The external magnetic field may not only activate the DE but it also accelerates the exciton relaxation to this state via spin relaxation. The absence of the observable PL might be also connected with polarization properties of the $0^{\rm L}$ DE emission. All phonon assisted mechanisms lead to the recombination polarized perpendicular to the c-axis of the NC which is suppressed by the local field effect in the prolate structures.[48]

In summary, we have developed a model that describes the radiative recombination of the DEs, which occurs as a result of the admixture of the DE to the bright exciton states via various physical mechanisms. The effects of the DE interaction with spins of dangling bonds at the NC surface and with acoustic and optical phonons, as well as an external magnetic field have been considered. We have shown that different activation mechanisms of the DE lead to different temperature dependences of its radiative recombination rate and different polarization properties.

Acknowledgment. Authors thank L. Biadala, M. Fernée, R. Vaxenburg, A. Shabaev, L. Boyer and D. Yakovlev for helpful discussions and TU Dortmund University for the hospitality. The work of A. V. R was supported by the Government of Russia (Project No. 14.Z50.31.0021, leading scientist M. Bayer), and by the Deutsche Forschungsgemeinschaft and the Russian Foundation of Basic Research (project 15-52-12015) in the frame of the ICRC TRR 160. Al.L.E. acknowledges the financial support of the Office of Naval Research (ONR) through the Naval Research Laboratory Basic Research Program and Alexander von Humboldt Foundation.

[1] R. S. Knox, *Theory of ecxitons* (Academic Press, New Yirk and London, 1963).
[2] C. R. L. P. N. Jeukens, P. C. M. Christianen, J. C. Maan, D. R. Yakovlev, W. Ossau, V. P. Kochereshko, T. Wojtowicz, G. Karczewski, and J. Kossut, Phys. Rev. B **66**, 235318 (2002).
[3] Yu. G. Kusrayev, B. P. Zakharchenya, G. Karczewski, T. Wojtowicz, and J. Kossut, Solid State Commun. **104**, 465 (1997) .
[4] M. Bayer, G. Ortner, O. Stern, A. Kuther, A. A. Gorbunov, A. Forchel, P. Hawrylak, S. Fafard, K. Hinzer, T. L. Reinecke, S. N. Walck, J. P. Reithmaier, F. Klopf, and F. Schäfer, Phys. Rev. B **65**, 195315 (2002).
[5] T. Smoleński,T. Kazimierczuk, M. Goryca, T. Jakubczyk,Ł Kłopotowski, Ł. Cywiński, P. Wojnar, A. Golnik, and P. Kossacki, Phys. Rev. B, **86**, 241305(R) (2012).
[6] M. Korkusinski and P. Hawrylak, Phys. Rev. B **87**, 115310 (2013).
[7] J. Puls, M. Rabe, H.-J. Wünsche, and F. Henneberger, Phys. Rev. B **60**, R16 303 (1999).
[8] F. Gindele, U. Woggon, W. Langbein, J. M. Hvam, M. Hetterich, and C. Klingshirn, Solid State Commun. **106**, 653 (1998).
[9] G. Sallen, A. Tribu, T. Aichele, R. Andre, L. Besombes, C. Bougerol, S. Tatarenko, K. Kheng, and J. Ph. Poizat, Phys. Rev. B **80**, 085310 (2009).
[10] M. Nirmal, D. J. Norris, M. Kuno, M. G. Bawendi, Al. L. Efros, and M. Rosen, Phys. Rev. Lett. **75**, 3728 (1995).
[11] Al. L. Efros, M. Rosen, M. Kuno, M. Nirmal, D. J. Norris, and M. G. Bawendi, Phys. Rev B **54**, 4843 (1996).
[12] M. Chamarro, C. Gourdon, P. Lavallard, O. Lublinskaya and A. I. Ekimov, Phys. Rev B **53**, 1336 (1996).
[13] Efros, Al. L. *Semiconductor and Metal Nanocrystals: Synthesis and Electronic and Optical Properties* edited by V. I. Klimov, Ch. 3, p. 103 (Marcel Dekker, New York, 2003).
[14] M. Califano, A. Franceschetti, and A. Zunger, Phys. Rev.

B **75**, 115401 (2007).
[15] M. Korkusinski, O. Voznyy, and P. Hawrylak, Phys. Rev. B **82**, 245304 (2010).
[16] A. Shabaev and AL. L. Efros, Nano lett. **4**, 1821 (2004).
[17] L. Biadala, F. Liu, M. D. Tessier, D. R. Yakovlev, B. Dubertret, and M. Bayer, Nano Lett. **14**, 1134 (2014).
[18] L. Biadala, B. Siebers, Y. Beyazit, M. D. Tessier, D. Dupont, Z. Hens, D. R. Yakovlev, and M. Bayer, ACS Nano, (published on line 18 February 2016).
[19] M. G. Bawendi, W. L. Wilson, L. Rothberg, P. J. Carroll, T. M. Jedju, M. L. Steigerwald, and L. E. Brus, Phys. Rev. Lett. **65**, 1623 (1990).
[20] M. Nirmal, C. B. Murray, and M. G. Bawendi, Phys. Rev. B **50**, 2293 (1994).
[21] M. G. Bawendi, P. J. Carroll, William L. Wilson, and L. E. Brus, The Journal of Chemical Physics **96**, 946 (1992).
[22] U. Woggon, F. Gindele, O. Wind, and C. Klingshirn, Phys. Rev. B 54, 1506 (1996).
[23] D. J. Norris, Al. L. Efros, M. Rosen, M. G. Bawendi, Phys. Rev. B **53**, 16347 (1996).
[24] F. J. P. Wijnen, J. H. Blokland, P. T. K. Chin, P. C. M. Christianen, and J. C. Maan, Phys. Rev. B **78**, 235318 (2008).
[25] A.G. del Águila, B. Jha, F. Pietra, E. Groeneveld, C. de Mello Donegá, J. C. Maan, D. Vanmaekelbergh, and P. C.M. Christianen, Acs Nano **8**, 5921 (2014).
[26] N. Le Thomas, E. Herz, O. Schöps, U. Woggon, and M.V. Artemyev, Phys. Rev. Lett. **94**, 016803 (2005).
[27] L. Biadala, Y. Louyer, Ph. Tamarat, and B. Lounis, Phys. Rev. Lett. **103**, 037404 (2009).
[28] L. Biadala, Y. Louyer, Ph. Tamarat, and B. Lounis, Phys. Rev. Lett. **105**, 157402 (2010).
[29] Y. Louyer, L. Biadala, J.-B. Trebbia, M. J. Fernée, Ph. Tamarat, and B. Lounis, Nano Lett. **11**, 4370 (2011).
[30] Y. Louyer, L. Biadala, Ph. Tamarat, and B. Lounis, Appl. Phys. Lett. **96**, 203111 (2010).
[31] M. J. Fernée, Ph. Tamarat, and B. Lounis, J. Phys. Chem. Lett. **4**, 609 (2013).
[32] E. Johnston-Halperin, D. D. Awschalom, S. A. Crooker, Al. L. Efros, M. Rosen, X. Peng, and A. P. Alivisatos, Spin Spectroscopy of Dark Excitons in Cdse Quantum Dots to 60 T, Phys. Rev. B **63**, 205309 (2001).
[33] S. A. Crooker, T. Barrick, J. A. Hollingsworth and V. I. Klimov, Appl. Phys. Lett. **82**, 2793 (2003).
[34] O. Labeau, P. Tamarat, and B. Lounis, Phys. Rev. Lett. **90**, 257404 (2003).
[35] M. Furis, J. A. Hollingsworth, V. I. Klimov, and S. A. Crooker, J. Phys. Chem. B **109**, 15332 (2005),
[36] C. de Mello Donega, M. Bode, and A. Meijerink, Phys. Rev. B **74**, 085320 (2006).
[37] D. Oron, A. Aharoni, C. de Mello Donega, J. van Rijssel, , A. Meijerink, and U. Banin, Phys. Rev. Lett. **102**, 177402 (2009).
[38] I. Moreels, G. Rain, R. Gomes, Z. Hens, T. Stoferle, M. Thilo, F. Rainer, Band-Edge Exciton Fine Structure of Small , Nearly Spherical Colloidal CdSe/ZnS Quantum Dots, ACS nano **5**, 8033 (2011).
[39] J.H. Blokland, V.I. Claessen, F.J.P. Wijnen, E. Groeneveld, C. de Mello Donegá, D. Vanmaekelbergh, A. Meijerink, J.C. Maan, and P.C.M. Christianen, Phys. Rev. B **83**, 035304 (2011).
[40] F. Liu, L. Biadala, A. V. Rodina, D. R. Yakovlev, D. Dunker, C. Javaux, J.-P. Hermier, A. L. Efros, B. Dubertret, and M. Bayer, Spin dynamics of negatively charged excitons in CdSe/CdS colloidal nanocrystals, Phys.Rev B **88**, 035302 (2013).
[41] F. Liu, A. V. Rodina, D. R. Yakovlev, A. Greilich, A. A. Golovatenko, A. S. Susha, A. L. Rogach, Yu. G. Kusrayev, and M. Bayer, Exciton spin dynamics of colloidal CdTe nanocrystals in magnetic fields, Phys. Rev. B **89**, 115306 (2014).
[42] M. Califano, A. Franceschetti, and A. Zunger, Nano Lett. **5**, 2360 (2005).
[43] K. Leung, S. Pokrant, and K. B. Whaley, Phys. Rev. B **57**, 12291 (1998).
[44] S. V. Goupalov, Phys. Rev. B **74**, 113305 (2006).
[45] A.V. Rodina and Al. L. Efros, Nano Letters **15**, 4214 (2015).
[46] M. S. Seehra, P. Dutta, S. Neeleshwar, Y.-Y. Chen, C. L. Chen, S. Wei Chou, C. C. Chen, and Chung-Li Dong, and Ching-Lin Chang, Adv. Mater. **20**, 1656 (2008).
[47] R. W. Meulenberg, J. R. I. Lee, S. K. McCall, K. M. Hanif, D. Haskel, J. C. Lang, L. J. Terminello, and T. van Buuren, J. Am. Chem. Soc. **131**, 6888 (2009).
[48] A. V. Rodina and Al. L. Efros, JETP **122**, no. 3 (2016) [ZhETF **149**, 641 (2016)].
[49] B. Siebers, L. Biadala, D. R. Yakovlev, A.V. Rodina, T. Aubert, Z. Hens, and M. Bayer, Phys. Rev. B **91**, 155304 (2015).
[50] S. A. Empedocles, R. Neuhauser, and M. G. Bawendi, Nature **399**, 126 (1999).
[51] C. Lethiec, J. Laverdant, H. Vallon, C. Javaux, B. Dubertret, J-M. Frigerio, C. Schwob, L. Coolen, and A. Maitre, Phys. Rev. X **4**, 021037 (2014).
[52] I. Chung, K. T. Shimizu, and M. G. Bawendi, Proc. Natl. Acad. Sci. U.S.A. **100**, 405 (2003).
[53] Al. L. Efros and A. V. Rodina, Solid State Commun. **72**, 645 (1989).
[54] A. I. Ekimov, F. Hache, M.C. Schanne-Klein, D. Ricard, C. Flytzanis, I. A. Kudryavtsev, T. V. Yazeva, A.V. Rodina, and Al. L. Efros, J. Opt. Soc. Am. B **10**, 100 (1993).
[55] A.V. Rodina and Al. L. Efros, Phys. Rev. B **82**, 125324 (2010).
[56] Al. L. Efros, A. I. Ekimov, F. Kozlowski, V. Petrova-Koch, H. Schmidbaur, and S. Shumilov, Solid State Commun. **78**, 853 (1991).
[57] Al.L. Efros, Phys. Rev. B **46**, 7448 (1992).
[58] S. V. Gupalov, I. A. Merkulov, Physics of the Solid State **41** 1349 (1999) [Fiz. Tverd. Tela **41**, 1473 (1999)].
[59] E. L. Ivchenko, *Optical Spectroscopy of Semiconductor Nannostructures* (Alpha Science International Ltd., Harrow, UK, 2005).
[60] A. I. Anselm, *Introduction to Semiconductor Theory* (Mir Publishers, Moscow, 1981).
[61] E. Yablonovitch, T. J. Gmitter, and R. Bhat, Phys. Rev. Lett. **61**, 2546 (1988).
[62] S. Schmitt–Rink, D. A. B. Miller, and D. S. Chemla, Phys. Rev. B **35**, 8113 (1987).
[63] L. D. Landau and E. M. Lifshitz,*Electrodynamics of Continuous Media* (Pergamon Press, Oxford, 1960).
[64] J. D. Jackson, *Classical Electrodynamics*, 3rd ed. (Wiley, New York, 1998).
[65] V. V. Batygin and I. N. Toptygin, *Sbornik zadach po elektrodinamike* 3rd ed. (Moscow, Nauka, 1970).
[66] There is error by factor 2 in the final expression for τ_0 in Refs. [11,13].
[67] The expression for the radiative recombination rate of the

DE stimulated by a magnetic field in Ref.11 contains a mistake.
[68] R. Englman and R. Ruppin, J. Phys. C **1**, 614 (1968).
[69] R. Ruppin, J. Phys. C **8**, 1969 (1975).
[70] H. Lamb, Proc. Math Soc. London **13**, 187 (1882).
[71] S. Nomura and T. Kobayashi, Sol. St. Commun. **82**, 335 (1992).
[72] M. C. Klein, F. Hache, D. Ricard, and C. Flytzanis, Phys. Rev. B **42**, 11123 (1990).
[73] T. Takagahara, J. Luminescence **70**, 129 (1996).
[74] B.L. Gel'mont, A.V. Rodina, Al. L. Efros, Sov. Phys. Semicond. **24**, 120 (1990).
[75] In the Ref. [21] the value $\rho = (I_\parallel - I_\perp)/(I_\parallel + 2I_\perp)$ was reported wich can be converted into the degree of linear polarization as $P_{\rm mem} = 3\rho/(\rho+2)$.
[76] C. Sinito, M. J. Fernée, S. V. Goupalov, P. Mulvaney, Ph. Tamarat, and B. Lounis, ACS Nano **8**, 11651 (2014).
[77] M. J. Fernée, C. Sinito, Ph. Tamarat, and B. Lounis, Nano Lett. **14**, 4480 (2014).
[78] A. R. Edmonds, *Angular momentum in Quantum mechanics*, (Princenton University Press, 1957).
[79] B. L. Gel'mont and M. I. D'yakonov, Fiz. Techn. Polupr **5**, 2191 (1971).
[80] L.D. Landau and E.M. Lifshitz, *Quantum Theory*, 2nd ed. (Pergamon, Oxford, 1965).
[81] S. V. Gupalov and E. L. Ivchenko, Phys. Sol. State **42**, 2030 (2000).
[82] Note, that expressions for the exciton wave functions in Refs.11,13,55 contain the phase factors i because of the different choice of the basis Bloch functions. In addition, the expressions for the ± 1 wave functions in Ref.11 contain a misprint.

Appendix

A. Exciton wave functions and energies

Calculations of the exciton fine structure require self consistent definitions of the band edge Bloch function and the electron and hole envelope functions. These definitions may include complex phases that were selected differently in various papers resulting sometimes in confusing or even wrong results. In spherical NCs additional complication arises from different definitions of the spherical functions that one can find in the literature. That is why in this Appendix we want to present explicit forms of the Bloch and envelope functions we use in the paper.

We chose the Bloch functions $u^{\rm c}_{1/2,\pm 1/2}$ of the Γ_6 conduction band and $u_{3/2,\mu}$ ($\mu = \pm 3/2, \pm 1/2$) of the Γ_8 valence band (point group T_d) according to Ref. [59]:

$$u^{\rm c}_{1/2,1/2} = S\uparrow, \quad u^{\rm c}_{1/2,-1/2} = S\downarrow, \tag{29}$$

and

$$\begin{aligned} u_{3/2,3/2} &= -\frac{1}{\sqrt{2}}(X+iY)\uparrow, \\ u_{3/2,-3/2} &= \frac{1}{\sqrt{2}}(X-iY)\downarrow, \\ u_{3/2,1/2} &= \frac{1}{\sqrt{6}}\left[-(X+iY)\downarrow + 2Z\uparrow\right], \\ u_{3/2,-1/2} &= \frac{1}{\sqrt{6}}\left[(X-iY)\uparrow + 2Z\downarrow\right]. \end{aligned} \tag{30}$$

Here S and X, Y, Z are the orbital Bloch functions for the s-type and p-type band edge symmetry, respectively. The spinor functions $\uparrow$ and $\downarrow$ are the eigen functions of the electron spin projection operator $s_z = \pm 1/2$.

The electron wave functions for the electron ground state $1S_{\rm e}$ level in spherical NC are

$$\Psi^{\rm e}_{\pm 1/2}(\mathbf{r}) = R_{\rm e}(r) Y_{00} u^{\rm c}_{1/2,\pm 1/2}, \tag{31}$$

where $Y_{00} = 1\sqrt{4\pi}$ and $R_{\rm e}(r)$ is the normalized radial function. The first size-quantization level of holes in a spherical NC is a $1S_{3/2}$ state[53,54] characterized by total angular momentum $J = 3/2$ and is four-fold degenerate with respect to its projection $M = 3/2, 1/2, -1/2, -3/2$ on the z axis. The wave functions of this state can be written in hole representation as[79]

$$\Psi^{\rm h}_M = 2\sum_{l=0,2}(-1)^{M-3/2}(i)^l R_l(r) \sum_{m+\mu=M} \begin{pmatrix} l & 3/2 & 3/2 \\ m & \mu & -M \end{pmatrix} Y_{l,m} u_{3/2,\mu}. \tag{32}$$

Here $\begin{pmatrix} i & k & l \\ m & n & p \end{pmatrix}$ are the Wigner 3 j -symbols, and the spherical angular harmonics Y_{lm} are defined in Ref. [78]. Note, that the factor $(i)^l$ is introduced because we use the definition of spherical harmonics Y_{lm} as given in Ref. [78] while in Ref. [79] the spherical harmonics were defined according to Ref. [80]. The radial wave functions R_0 and R_2 in Eq. (32) are normalized as $\int (R_0^2 + R_2^2) r^2 dr = 1$ and satisfy the system of radial equations that can found in Refs. [55,79].

The effective electron–hole exchange interaction between confined electrons and holes can be written as

$$\hat{H}_{\rm exch} = -\eta(\boldsymbol{\sigma}^{\rm e}\boldsymbol{J}), \tag{33}$$

where the effective constant η may include both short–range and long–range contributions.[11,13,44,55,81] With account of the short–range contribution only it is given by

$$\eta = \frac{a_0^3}{6\pi}\varepsilon_{\rm exch}\int_0^\infty dr r^2 R_{\rm e}^2(r)[R_0^2(r) + 0.2R_2^2(r)], \tag{34}$$

where a_0 is the lattice constant and $\varepsilon_{\rm exch}$ is the exchange constant. The integral in Eq. (34) depends on the ratio of light to heavy hole effective masses, β , and

is inversely proportional to the a^3 in the case of impenetrable confined potential of NC with radius a. In CdSe the exchange constant was extracted from the bulk exciton splitting: $\varepsilon_{\rm exch} = 450$ meV.[11]

The electron–hole exchange interaction splits the eight fold exciton state into states with total momentum $\mathcal{F} = 2$ (dark ground state with the energy $-3\eta/2$) and $\mathcal{F} = 1$ (bright state with the energy $+5\eta/2$). The exciton wave functions with total momentum $\mathcal{F}$ and projection F can be constructed in the electron-hole representation using general rule:

$$\Psi^{\rm ex}_{\mathcal{F},F} = \sqrt{2\mathcal{F}+1}\,(-1)^{F-1} \sum_{m+\mu=M}\sum_{m+M=F} \begin{pmatrix} 1/2 & 3/2 & \mathcal{F} \\ m & M & -F \end{pmatrix} \Psi^{\rm e}_m \Psi^{\rm h}_M \,. \quad (35)$$

In explicit form the exciton wave functions are:

$$\begin{aligned} \Psi^{\rm ex}_{2,\pm 2} &= \Psi^{\rm e}_{\pm 1/2}\Psi^{\rm h}_{\pm 3/2}\,, \\ \Psi^{\rm ex}_{2,\pm 1} &= \frac{1}{2}\Psi^{\rm e}_{\mp 1/2}\Psi^{\rm h}_{\pm 3/2} + \frac{\sqrt{3}}{2}\Psi^{\rm e}_{\pm 1/2}\Psi^{\rm h}_{\pm 1/2}\,, \\ \Psi^{\rm ex}_{2,0} &= \frac{1}{\sqrt{2}}\left[\Psi^{\rm e}_{\pm 1/2}\Psi^{\rm h}_{\mp 1/2} + \Psi^{\rm e}_{\mp 1/2}\Psi^{\rm h}_{\pm 1/2}\right] \end{aligned} \quad (36)$$

for $\mathcal{F} = 2$ and

$$\begin{aligned} \Psi^{\rm ex}_{1,\pm 1} &= \mp\frac{\sqrt{3}}{2}\Psi^{\rm e}_{\mp 1/2}\Psi^{\rm h}_{\pm 3/2} \pm \frac{1}{2}\Psi^{\rm e}_{\pm 1/2}\Psi^{\rm h}_{\pm 1/2}\,, \\ \Psi^{\rm ex}_{1,0} &= \frac{1}{\sqrt{2}}\left[\Psi^{\rm e}_{\pm 1/2}\Psi^{\rm h}_{\mp 1/2} - \Psi^{\rm e}_{\mp 1/2}\Psi^{\rm h}_{\pm 1/2}\right] \end{aligned} \quad (37)$$

for $\mathcal{F} = 1$.

The spherical symmetry can be broken by the internal hexagonal crystal field in semiconductors with wurtzite structure (such as CdSe) and the non-spherical, ellipsoidal shape of NCs, which splits the $\pm 1/2$ and $\pm 3/2$ hole sublevels. The action of the total anisotropic field can be written as

$$\hat{H}^{\rm an} = (\Delta/2)\left[5/4 - M^2\right]. \quad (38)$$

This perturbation shifts the energies of exciton states with $F = 0$ and $|F| = 2$ by $\pm\Delta/2$ without modification of their wave function and mixes the states with $|F| = 0$ with different $\mathcal{F}$. The resulting energies of the Hamiltonian $\hat{H}_{\rm fine} = \hat{H}_{\rm exch} + \hat{H}^{\rm an}$ that is defined in Eq. (1)) are:[11]

$$\begin{aligned} \epsilon_2 &= -3\eta/2 - \Delta/2\,, \\ \epsilon_1^{\rm U,L} &= \eta/2 \pm \sqrt{f^2+d}\,, \\ \epsilon_0^{\rm U,L} &= \eta/2 + \Delta/2 \pm 2\eta\,. \end{aligned} \quad (39)$$

Here U and L correspond to "+" and "-" signs in the equations for the upper and lower states, respectively, $f = (-2\eta+\Delta)/2$ and $d = 3\eta^2$. The exciton wave functions in the electron-hole representation are:[82]

$$\begin{aligned} \Psi_{-2}(\boldsymbol{r}_{\rm e},\boldsymbol{r}_{\rm h}) &= \Psi_{\downarrow,-3/2}(\boldsymbol{r}_{\rm e},\boldsymbol{r}_{\rm h})\,, \\ \Psi_{2}(\boldsymbol{r}_{\rm e},\boldsymbol{r}_{\rm h}) &= \Psi_{\uparrow,3/2}(\boldsymbol{r}_{\rm e},\boldsymbol{r}_{\rm h})\,, \\ \Psi_0^{\rm U,L}(\boldsymbol{r}_{\rm e},\boldsymbol{r}_{\rm h}) &= \frac{1}{\sqrt{2}}\left[\Psi_{\uparrow,-1/2}(\boldsymbol{r}_{\rm e},\boldsymbol{r}_{\rm h}) \mp \Psi_{\downarrow,1/2}(\boldsymbol{r}_{\rm e},\boldsymbol{r}_{\rm h})\right]\,, \\ \Psi_1^{\rm U}(\boldsymbol{r}_{\rm e},\boldsymbol{r}_{\rm h}) &= C^+\Psi_{\uparrow,1/2}(\boldsymbol{r}_{\rm e},\boldsymbol{r}_{\rm h}) - C^-\Psi_{\downarrow,3/2}(\boldsymbol{r}_{\rm e},\boldsymbol{r}_{\rm h})\,, \\ \Psi_1^{\rm L}(\boldsymbol{r}_{\rm e},\boldsymbol{r}_{\rm h}) &= C^-\Psi_{\uparrow,1/2}(\boldsymbol{r}_{\rm e},\boldsymbol{r}_{\rm h}) + C^+\Psi_{\downarrow,3/2}(\boldsymbol{r}_{\rm e},\boldsymbol{r}_{\rm h})\,, \\ \Psi_{-1}^{\rm U}(\boldsymbol{r}_{\rm e},\boldsymbol{r}_{\rm h}) &= C^-\Psi_{\uparrow,-3/2}(\boldsymbol{r}_{\rm e},\boldsymbol{r}_{\rm h}) - C^+\Psi_{\downarrow,-1/2}(\boldsymbol{r}_{\rm e},\boldsymbol{r}_{\rm h})\,, \\ \Psi_{-1}^{\rm L}(\boldsymbol{r}_{\rm e},\boldsymbol{r}_{\rm h}) &= C^+\Psi_{\uparrow,-3/2}(\boldsymbol{r}_{\rm e},\boldsymbol{r}_{\rm h}) + C^-\Psi_{\downarrow,-1/2}(\boldsymbol{r}_{\rm e},\boldsymbol{r}_{\rm h})\,, \end{aligned} \quad (40)$$

where $\Psi_{\uparrow,M}(\boldsymbol{r}_{\rm e},\boldsymbol{r}_{\rm h}) = \Psi^{\rm e}_{+1/2}\Psi^{\rm h}_M$ and $\Psi_{\downarrow,M}(\boldsymbol{r}_{\rm e},\boldsymbol{r}_{\rm h}) = \Psi^{\rm e}_{-1/2}\Psi^{\rm h}_M$, and

$$C^{\pm} = \sqrt{\frac{\sqrt{f^2+d}\pm f}{2\sqrt{f^2+d}}}\,. \quad (41)$$

For the chosen basis, the Kane matrix element is defined as $P = -i\langle S|\hat{p}_x|X\rangle = -i\langle S|\hat{p}_y|Y\rangle = -i\langle S|\hat{p}_z|X\rangle$, where $\hat{\boldsymbol{p}} = -i\hbar\nabla$. The square of the overlap integral between the electron and hole wave functions is defined in Ref.11: $K = \left|\int dr r^2 R_e(r)R_0(r)\right|^2$.

B. Details of the radiative rate calculations for the $0^{\rm L}$ DE.

Using the exciton wave functions we find the mixing of the $0^{\rm L}$ DE state with different bright excitons by perturbations $\hat{V}_{\rm e}$ and $\hat{V}_{\rm h}$:

$$\begin{aligned} &\langle -1^{\rm U,L}|\hat{V}_{\rm e}|0^{\rm L}\rangle = \mp\frac{C^{\pm}}{\sqrt{2}}V_{\rm e}^*\,, \quad \langle +1^{\rm U,L}|\hat{V}_{\rm e}|0^{\rm L}\rangle = \frac{C^{\pm}}{\sqrt{2}}V_{\rm e}\,, \\ &\langle -1^{\rm U,L}|\hat{V}_{\rm h}|0^{\rm L}\rangle = \frac{C^{\mp}}{\sqrt{2}}V_{\rm h,1}^* \mp \frac{C^{\pm}}{\sqrt{2}}V_{\rm lh}^*\,, \\ &\langle +1^{\rm U,L}|\hat{V}_{\rm h}|0^{\rm L}\rangle = \mp\frac{C^{\mp}}{\sqrt{2}}V_{\rm h,1} + \frac{C^{\pm}}{\sqrt{2}}V_{\rm lh}\,, \\ &\langle 0^{\rm U}|\hat{V}_{\rm e}+\hat{V}_{\rm h}|0^{\rm L}\rangle = \frac{1}{2}(V_{\uparrow,-1/2} - V_{\downarrow,1/2})\,. \end{aligned} \quad (42)$$

One can see from Eq. (42), that the $0^{\rm L}$ DE state can be activated by the $V_{\rm lh}$ matrix element that is responsible for the flip of the light hole spin, in contrast to the ± 2 DE (see for comparison Eq.(10)). In addition, the diagonal matrix elements $V_{\uparrow,-1/2} - V_{\downarrow,1/2}$ couple the bright and the DE with $F = 0$ without changing their spin projection.

Assuming again that all perturbation matrix elements are smaller than the exciton fine structure splittings, one can find the resulting dipole transition matrix elements for the $0^{\rm L}$ DE in the framework of second order pertur-

bation theory as

$$|d_{\parallel}^{0\mathrm{L}}|^2 = \frac{|d_0|^2}{4}\frac{|V_{\uparrow,-1/2}-V_{\downarrow,1/2}|^2}{(\tilde{\varepsilon}_0^{\mathrm{U}}-\tilde{\varepsilon}_0^{\mathrm{L}})^2}, \quad (43)$$

$$d_x^{0\mathrm{L}} = d_{+1}^{0\mathrm{L}} + d_{-1}^{0\mathrm{L}}, \quad d_y^{0\mathrm{L}} = -i(d_{+1}^{0\mathrm{L}} - d_{-1}^{0\mathrm{L}}),$$

$$d_{+1}^{0\mathrm{L}} = \frac{d_{+1}^{\mathrm{U}}}{\sqrt{2}}\frac{(C^+V_{\mathrm{e}} - C^-V_{\mathrm{h},1} + C^+V_{\mathrm{lh}})}{\tilde{\varepsilon}_{+1}^{\mathrm{U}}-\tilde{\varepsilon}_0^{\mathrm{L}}} + \frac{d_{+1}^{\mathrm{L}}}{\sqrt{2}}\frac{(C^-V_{\mathrm{e}} + C^+V_{\mathrm{h},1} + C^-V_{\mathrm{lh}})}{\tilde{\varepsilon}_{+1}^{\mathrm{L}}-\tilde{\varepsilon}_0^{\mathrm{L}}},$$

$$d_{-1}^{0\mathrm{L}} = \frac{d_{-1}^{\mathrm{U}}}{\sqrt{2}}\frac{(-C^+V_{\mathrm{e}}^* + C^-V_{\mathrm{h},1}^* - C^+V_{\mathrm{lh}}^*)}{\tilde{\varepsilon}_{-1}^{\mathrm{U}}-\tilde{\varepsilon}_0^{\mathrm{L}}} + \frac{d_{-1}^{\mathrm{L}}}{\sqrt{2}}\frac{(C^-V_{\mathrm{e}}^* + C^+V_{\mathrm{h},1}^* + C^-V_{\mathrm{lh}}^*)}{\tilde{\varepsilon}_{-1}^{\mathrm{L}}-\tilde{\varepsilon}_0^{\mathrm{L}}}. \quad (44)$$

Here the bright exciton matrix elements are (see also Eq. (4))

$$d_{\pm1}^{\mathrm{U}} = \mp\frac{d_0}{2\sqrt{2}}\left(C^+ + \sqrt{3}C^-\right),$$
$$d_{\pm1}^{\mathrm{L}} = \frac{d_0}{2\sqrt{2}}\left(\sqrt{3}C^+ - C^-\right), \quad (45)$$

and the exciton energies $\tilde{\varepsilon}_0^{\mathrm{U}}$, $\tilde{\varepsilon}_{\pm1}^{\mathrm{U,L}}$ and $\tilde{\varepsilon}_{\pm2}$ may differ from the unperturbed exciton energies $\varepsilon_0^{\mathrm{U}}$, $\varepsilon_1^{\mathrm{U,L}}$ and ε_2 by the energy of the phonons or dangling bond spin states participating in the transition as well as by the Zeeman level energies in an external magnetic field. Straight forward calculations show that in the case $\tilde{\varepsilon}_1^{\mathrm{U,L}} - \tilde{\varepsilon}_0^{\mathrm{L}} = \varepsilon_1^{\mathrm{U,L}} - \varepsilon_0^{\mathrm{L}} = -\Delta/2 + 2\eta \pm \sqrt{f^2+d}$ the coupling between bright and dark excitons mediated by $V_{\mathrm{h},1}$ results in the superposition of the 1^{L} and 1^{U} bright states, which contributions in the radiative decay is destructive and does not lead to the activation of the DE recombination. In the contrast, V_{e} and V_{lh} mediated coupling with bright excitons does lead to the 0^{L} DE activation.

Using the above calculated matrix elements for the perturbation induced by an external magnetic field $\boldsymbol{B} = (B_x, B_y, B_z)$, one can calculate the magnetic field induced radiative decay rate of the 0^{L} DE as

$$\Gamma_B = \Gamma_B^{00} + \Gamma_B^{01}, \quad (46)$$

where the rate

$$\Gamma_B^{00} = \frac{1}{4\tau_0}\frac{[\mu_{\mathrm{B}}(g_{\mathrm{e}}+g_{\mathrm{h}})B\cos\Theta]^2}{16\eta^2} \quad (47)$$

is mediated by the DE coupling with 0^{U} bright exciton and the rate

$$\Gamma_B^{01} = \frac{|V_{\mathrm{e}}+V_{\mathrm{lh}}|^2}{4\eta^2}\frac{1}{R\tau_0} = \frac{[\mu_{\mathrm{B}}(g_{\mathrm{e}}-2g_{\mathrm{h}})B\sin\Theta]^2}{16\eta^2}\frac{1}{R\tau_0}. \quad (48)$$

is mediated by the DE coupling with $\pm1^{\mathrm{U,L}}$ bright excitons. We note again, that the rate of radiative recombination Γ_B does not depend on the splitting between $\pm1/2$ and $\pm3/2$ hole states, Δ.

The polarization properties of the PL from the 0^{L} DE activated by a magnetic field are determined by the DE coupling with both the $\pm1^{\mathrm{L,U}}$ and 0^{U} bright excitons. The activation processes are shown schematically in Fig. 3(a) by the blue and red lines for the $\pm1^{\mathrm{L,U}}$ mediated and 0^{U} mediated coupling, respectively. As expected, the 0^{U} mediated PL is linearly polarized parallel to the c-axis and the respective dipole transition element $d_{\parallel}^{0\mathrm{L}} \propto B_z$. The coupling of 0^{L} DE with $+1^{\mathrm{L,U}}$ and $-1^{\mathrm{L,U}}$ leads to a coherent superposition of these two intermediate states, contributing to the PL in second order perturbation theory. The transition dipole elements $d_{+1}^{0\mathrm{L}}$ and $d_{-1}^{0\mathrm{L}}$ of these coherent states, which modules are equal to each other (see Eq. (44)), result in the linearly polarized PL with dipoles $d_{x,y} \propto B_{x,y}$. In the case when the magnetic field is either parallel or perpendicular to the c-axis ($B_{x,y} = 0$ or $B_z = 0$, respectively), the PL is linearly polarized along the magnetic field.

The dangling bond assisted recombination of the 0^{L} DE may occur also via the coupling with $\pm1^{\mathrm{L,U}}$ or with 0^{U} bright excitons, and the resulting recombination rate can be written as $\Gamma_{\mathrm{db}} = \Gamma_{\mathrm{db}}^{01} + \Gamma_{\mathrm{db}}^{00}$. The spin flip of the dangling bonds provides coupling of the 0^{L} DE with the $\pm1^{\mathrm{L,U}}$ bright excitons. This mechanism leads to the radiative recombination rate

$$\Gamma_{\mathrm{db}}^{01} = \frac{\alpha^2}{2\eta^2}\frac{N_{\mathrm{db}}}{R\tau_0}. \quad (49)$$

The diagonal part $-\alpha\sum_j \sigma_z^{\mathrm{e}}\sigma_z^j$ of the exchange Hamiltonian (20) provides the coupling of the 0^{L} DE with the 0^{U} bright exciton via $|V_{\uparrow,-1/2} - V_{\downarrow,1/2}|^2 = \alpha^2|\sum_j\langle\sigma_z^j\rangle^2|$ and leads to the following recombination rate

$$\Gamma_{\mathrm{db}}^{00} = \frac{\alpha^2}{16\eta^2}\left[N_{\mathrm{db}}(N_{\mathrm{db}}-1)\rho_{\mathrm{db}}^2 + N_{\mathrm{db}}\right]\frac{1}{R\tau_0}, \quad (50)$$

where $\rho_{\mathrm{db}} = -\sum_j\langle\sigma_z^j\rangle/N_{\mathrm{db}}$. One can see from Eq.(50), that $\Gamma_{\mathrm{db}}^{00}$ depends strongly on polarization of the dangling bond spins. In Ref. 45 we have considered the formation of the magnetic polaron state via optical pumping of the dangling bond spins during the dangling bond assisted recombination of the ±2 DE. Such dynamic polarization of the dangling bond spins is not possible in the case of the 0^{L} DE recombination, however the dangling bond polarization ρ_{db} can be created by other means. In contrast to the dangling bond assisted recombination of the ±2 DE, the polarization of the dangling bond spins increases the rate of the 0^{L} DE radiative recombination.

The dangling bond assisted activation of the DE and PL polarization connected with this activation are shown schematically in Fig. 3(b). The flip of the dangling bond spin leads to different initial or final states of the NC for the σ^+ and σ^- polarized transitions as well as for the c-polarized transitions. Therefore probabilities of the radiative recombination via these independent channels can be directly added up and the PL polarization of the DE is a mixture of the linear polarization along c-axis and circular polarization perpendicular to the c-axis.

Our calculations show that phonons couple the $0^{\,\mathrm{L}}$ DE only with $\pm 1^{\mathrm{L,U}}$ bright excitons. The resulting radiative recombination rate at the energies $E_{\mathrm{F}} \mp E_{\mathrm{ph}}$ can be written:

$$\Gamma_{\mathrm{ph}}^{01}(E_{\mathrm{F}} \mp E_{\mathrm{ph}}) = \frac{3V_{\mathrm{ph}}^2 E_{\mathrm{ph}}^2}{(-\Delta\eta \pm E_{\mathrm{ph}}(-\Delta + 4\eta) + E_{\mathrm{ph}}^2)^2} \frac{N_{\mathrm{B}} + 1/2 \pm 1/2}{4R\tau_0} \,. \tag{51}$$

The activation processes are shown schematically in Fig. 3(c) for the PL which is accomplishing by the phonon emission. In the prolate CdSe NCs, where the $0^{\,\mathrm{L}}$ DE is the ground exciton level, one cannot neglect the phonon energy in Eq. (51) for both the acoustic and optical phonons. The resulting dipole transition elements and recombination rates for the acoustic phonon assisted transitions, which account of both Stokes and anti- Stokes components of PL, and for the optical phonon assisted transitions, which account of only the Stokes components of PL are given in Table II.